University of Southampton

Department of Mechanical Engineering

THE EFFECTS OF PRE-STRAIN, BOTH UNIDIRECTIONAL AND CYCLIC ON THE SUBSEQUENT PRECIPITATION HARDENING AND FATIGUE BEHAVIOUR OF ALUMINIUM ALLOY

by

John H. Havelock

Thesis submitted for

the

Degree of Master of Philosophy

April 1975

ABSTRACT

FACULTY OF ENGINEERING AND APPLIED SCIENCE

DEPARTMENT OF MECHANICAL ENGINEERING

MASTER OF PHILOSOPHY

THE EFFECTS OF PRE-STRAIN, BOTH UNIDIRECTIONAL AND CYCLIC ON THE SUBSEQUENT PRECIPITATION HARDENING AND FATIGUE BEHAVIOUR OF ALUMINIUM ALLOY.

by John H.Havelock.

Abstract

Aluminium alloy Hiduminium RR58 in the solution treated condition has been subjected to (a) stretching, and (b) cyclic straining, at room temperature before subsequent ageing treatment; its fatigue properties and the micro and macro structure after ageing have been compared with unstretched aged material.

Macroscopic fracture surface examination has been carried out on reverse bend fatigue specimens.

Scanning electron microscopy has been used to examine the fracture surfaces of rotating-bending-fatigue specimens.

Thin foil electron microscopy has been used to examine the condition of the material used for the fatigue tests.

It was found that precipitation occurred on dislocations introduced by pre-strain prior to ageing and that in the cyclically strained material a substructure was formed.

At the stress level chosen for comparison with the material which had not been pre-strained it was found that unidirectional pre-strain (tensile) prior to ageing improved the fatigue properties but that the cycling pre-strain (R = -1) was detrimental to the fatigue properties. Both subgrain boundary and grain boundary fatigue cracks occurred in the cyclically pre-strained material.

Summary

Aluminium alloy Hiduminium RR58 is used in the forged, sheet and plate forms under slightly varying compositions in the supersonic aircraft Concorde.

During production of the sheet or plate it is usually found that the material has distortions introduced by the quenching operation of the solution treatment.

The material is stretched in this soft condition to remove these distortions prior to the subsequent ageing treatment.

It has been reported that the plastic stretching (unidirectional strain) changes the microstructure developed by subsequent ageing treatment and alters the mechanical properties of the fully aged alloy.

Precipitation occurs on the dislocation nuclei introduced by the stretch. Cyclic pre-strain before age hardening was thought to be possibly more effective in nucleating precipitates than unidirectional strain.

The following investigation was carried out by taking RR58 in the solution treated condition and subjecting separate bulk samples to no stretching (Zero cycle), unidirectional stretch ($\frac{1}{4}$ cycle), 3 full cycles and 1000 full cycles before age hardening to the specification condition 19 hours at 190° C. The unidirectional stretch was at a stress of 262.5 MN/m^2 (17 $tonf/in^2$) and the cycling stresses at $\pm$ 262.5 MN/m^2 ($\pm$ 17 $tonf/in^2$) (R = -1).

Stretching and cycling loads prior to ageing were applied to the bulk samples using a LOSENHAUSEN UHP 600 KN machine for which a special load cycling attachment had been devised and built. Each sample of bulk material was then cut and machined to make sets of Rolls-Royce-type fatigue specimens.

Fatigue testing in rotating bending was carried out to produce an S/N curve for the quarter cycle (unidirectional stretch) material and comparative values at a chosen stress level (232 MN/m^2) were obtained for no stretch, 3 full cycles and the 1000 full cycles material. The differences in fatigue life were evaluated by a statistical method.

Fractographic examination of the fractured rotating bending specimens was carried out using an electron scanning microscope. In addition to the rotating bending fatigue tests on Rolls Royce type specimens, flat strip specimens were taken from the unidirection stretch, 3 cycle and 1000 cycle bulk material after ageing and these were fatigue tested in reverse bending using an Avery/Carl Schenck-type machine in order that macro and fractographic examination of fatigue fractures could be made.

The susceptibility of the unidirectional stretch ($\frac{1}{4}$ cycle) material to ageing time was examined by the heat treatment of samples from 13 to 57 hours followed by Rockwell and Vickers hardness tests.

The electrical conductivity of the various heat treated samples was also investigated using a Novamho Type 101 apparatus. Microfoils were prepared of the $\frac{1}{4}$ cycle, 3 cycle, 1000 cycle and zero cycle aged material and these were examined in the electron microscope.

It was found that precipitation occurred on dislocations introduced by pre-strain prior to ageing and that in the cyclically strained material a substructure was formed.

At the stress level chosen for comparison with the material which had not been pre-strained it was found that unidirectional pre-strain (tensile) prior to ageing improved the fatigue properties but that the cycling pre-strain (R = -1) was detrimental to the fatigue properties. Both subgrain boundary and grain boundary fatigue cracks occurred in the cyclically pre-strained material.

ACKNOWLEDGEMENTS

The author gratefully acknowledges the valuable guidance and continuous technical advice given by his supervisors Drs. T.R.G. Williams and P.J.E. Forsyth, without which this work would not have been possible.

The facilities of the Materials Laboratories at the University were kindly made available by Professor R.L. Bell.

Facilities at the Royal Aircraft Establishment Farnborough and the help from Mr. C. Peel on electron microscopy, were much valued.

The facilities of the Materials Laboratories at Bournemouth College of Technology were kindly made available by the Principal Dr. R.B. Bailey.

Assistance given by the technical staff at laboratories is much appreciated.

TABLE OF CONTENTS

CHAPTER 1

INTRODUCTION

Aluminium alloy Hiduminium RR58 was developed originally as an engine material capable of service at elevated temperatures. The composition was optimised to produce good creep resistance at 175 - 250°C in the forged alloy.

The advent of the Concorde Supersonic Transport application demanded a structural aluminium alloy required to withstand a long service life at temperatures significantly below the range in which RR58 had been used satisfactorily for many years. For this very critical application it was necessary to make certain modifications to both composition and production methods to produce a material that would satisfy the design requirements. This has involved a considerable amount of research and the present Concorde specifications represent the optimised version of this alloy where creep resistance has been of primary concern.

It should be realised that as with most specifications the aircraft manufacturers demand preferred composition limits which certainly on some elements are considerably narrower than indicated in the specification.

For example although the specification range for Cu is 1.8 - 2.7% as shown in Table 1A most Concorde material would be within the composition range shown in Table 1B. This point is particularly mentioned because it will be seen that the composition chosen for this research has low copper, and although it is still within the main specification it is not within the manufacturers preferred range and therefore would be unlikely to meet the more stringent creep requirements. Nevertheless it was chosen for this work as being a suitable composition to respond to the pre-strain conditions that would be applied.

SPECIFICATIONS FOR THE COMPOSITION OF RR58 ALLOYS are:-

TABLE 1

	1A Concord material specification		1B Material range most suitable for manufacturer		1C Composition used for present tests	
	min. wt.%	max. wt.%	min. wt.%	max. wt.%	min. wt.%	max. wt.%
Cu	1.8	2.7	2.25	2.7	1.88	
Mg	1.2	1.8	1.35	1.65	1.74	
Ni	0.8	1.4	1.0	1.3	1.12	
Fe	0.9	1.4	0.9	1.2	0.99	
Si	0.15	0.25	0.18	0.25	0.14	
Ti		0.2		0.2		
Zn		0.1				
Pb		0.05				
Sn		0.05				
Al	remainder		remainder		remainder	

Aluminium alloy Hiduminium RR58 to the preferred composition shown in Table 1B is used extensively for the Concorde structure in a variety of forms, plate, sheet, extrusions and forgings. The specifications require that plate and sheet be stretched (1.5 - 2.5%) in order to remove distortion and relieve the residual stresses. This is done after solution treatment i.e. in the soft condition before it is artificially age hardened.

Composition of the alloy, heat treatment procedure and prior cold work can considerably alter the subsequent ageing rate but in practice these variables are closely controlled. The present programme of work was undertaken to evaluate the effect of unidirectional pre-strain and of cyclic pre-strain (R = -1) introduced between solution treatment and artificial ageing on (1) Fatigue life (2) Alloy structure.

There is evidence that cyclic pre-strain before ageing can produce

more effective precipitation nuclei than results from unidirectional pre-strain[17] and that static strength is improved. The aim of the present work was to use these effects to produce improvements in fatigue properties of the alloy. It was considered that prior fatigue (cyclic pre-strain) of the alloy in the solution treated condition would produce precipitation nuclei in those regions where strengthening would be most beneficial in resisting subsequent fatigue deformation. In order to produce as uniform a fatigue strain (pre-strain) as possible in the alloy it was decided to apply 1% cyclic strain and this same value was used for the unidirectional strain applied to the control specimens.

CHAPTER 2

REVIEW OF CONSTITUTION AND AGEING CHARACTERISTICS OF RR58 TYPE ALLOYS

Figure 1 shows the relevant part of the Al-Cu-Mg phase diagram within which the RR58 compositions are situated. RR58 has approximately an equiatomic ratio of Cu and Mg and may be considered as belonging to the pseudo binary system α + S phase whereas the usual duralumin compositions that have about 4% Cu and $<$ 1% Mg by weight are α + θ phase alloys.

Various studies have indicated the ageing sequence for these pseudo binary alloys representing RR58 and will now be summarised.

2.1 Stage one hardening is associated with the formation of G P B zones which are ordered clusters of copper and magnesium coherent with the matrix. Above 190°C Silcock[1] found zones richer in copper (S") and she called these G P B2zones and has suggested that these are related to the compound $Mg_2Cu_5Al_5$.

2.2 Stage two hardening is associated with precipitation of S' whilst G P B zones persist. Precipitation of S' also occurs on dislocation lines generated in the quenching operation, or by cold work before ageing.[2]

The S' phase has the same structure as S but its presence is distinguished from it detected by slight streaking and distortion of the precipitate electron diffraction spots.[6]

Prolonged ageing results in the disappearance of the G P B zones and the growth of S' and its transformation to S precipitate resulting in softening.

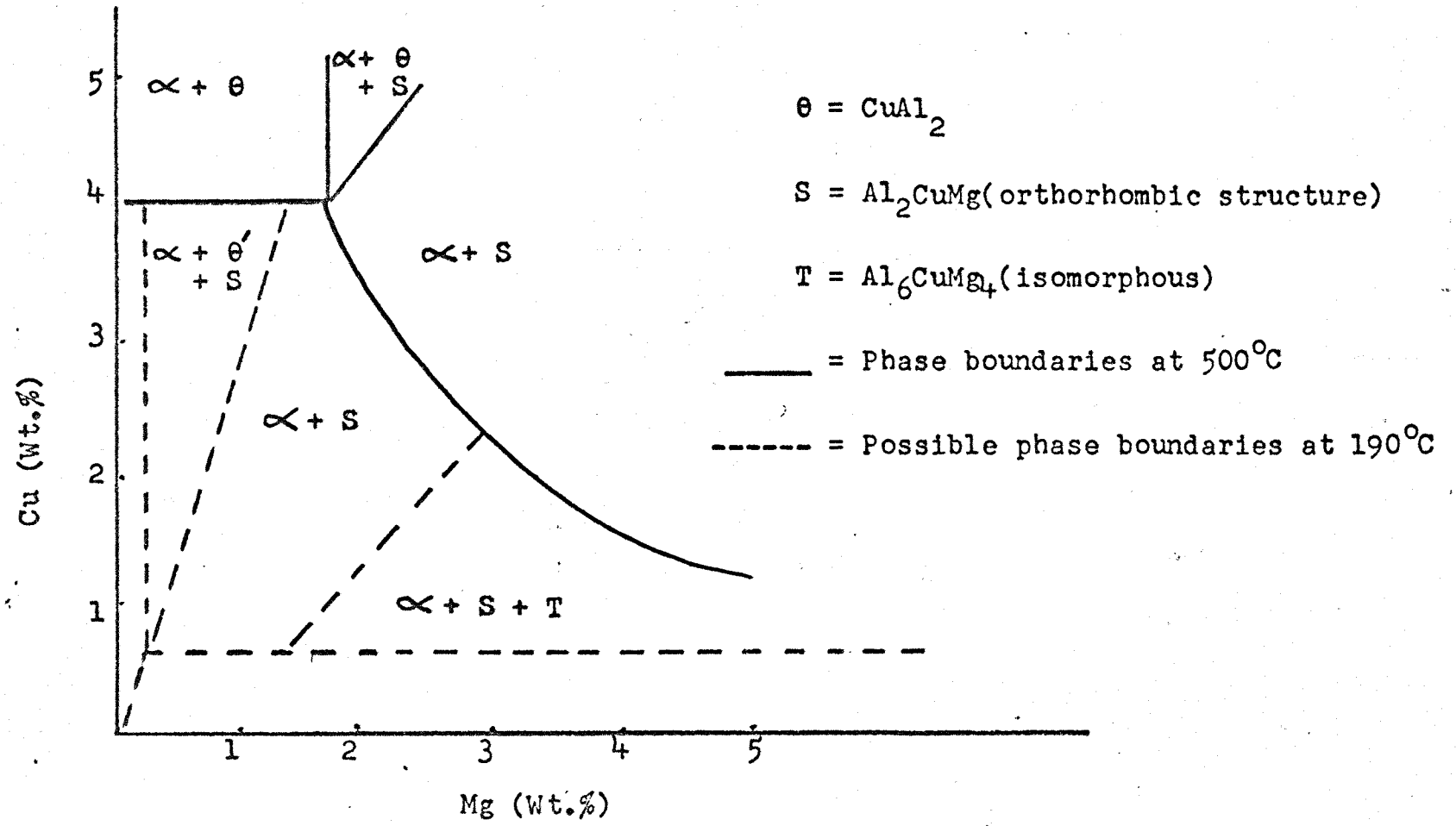

FIG. 1 PHASE DIAGRAM FOR TERNARY Al-Cu-Mg SYSTEM

(after Weatherley, Little, Silcock)

Small amounts of cold work before ageing produce increased age-hardening in a wide range of ternary Al-Cu-Mg alloys.[2,3] The transition from zones to S precipitate is accelerated by deformation since more favourable sites for S nucleation have been provided.

As the result of cold work between solution treatment and artificial ageing the driving energy of the ageing process is increased, and homogeneous growth of G P B zones and their transformation to S' in the matrix occurs slowly whilst a more rapid heterogeneous direct precipitation of S' and its transformation to the non-coherent S phase occurs at grain boundaries and on dislocations.

In all quenched alloys there is a high density of dislocation lines in quench bands and as loops and elongated helices dispersed throughout the grains. The appearance of the loops and helices and the relative densities are associated with the excess vacancy content.[4,5] The higher energy from cold working leads to the formation of helices whereas these are less likely to be generated in quenched alloys without prior cold work.

2.3 G P B Zones

The composition used for this work contains α + S in equilibrium and will follow the ageing sequence described above. G P B zones appear in such an alloy.

Silcock[1] examined Al-Cu-Mg alloys of Cu : Mg ratios 2.2 : 1 by weight and she suggested that the G P B zones were needle shaped zones of length 40 - 80 A^{o} and diameter 10 - 20 A^{o} with a possible face centred tetragonal cell with a=b = 5.5 A^{o} and C = 4.04 A^{o}.

Zones were in the $\langle 001 \rangle$ directions in the aluminium matrix. The structure of the zones was suggested as based on the compound $Mg_2Al_5Cu_5$.

The zones increase in size with increasing ageing time and temperature.

Gerold & Haberkorn[7] considered the structure as ordered and consisting of small spherical zones approx. 16 A^{o} diameter.

Zones found in alloys of high Cu : Mg ratios (3 : 1) are not G P B but are predominantly the same as G P zones found in binary Al-Cu alloys. Needle shaped zones are found in Al-Mg-Si alloys[8,9] and ordered spherical zones in Al-Mg-Zn alloys.

Nabarro[10] showed that a disc is a minimum energy shape for a highly strained precipitate. The habit plane of the disc should be 100 if anisotropic elasticity is taken into account and this is so for F.C.C. alloys except Al-Zn.

Needle shaped zones have more strain energy than a disc but less than a sphere.

The alloy used in the tests contained 0.14% Si.

Wilson, Moore and Forsyth[11] reported that silicon decreased the rate of formation of G P B zones, but the coherency strain associated with the formation is increased, resulting in increased hardening. Cold working the solution treated RR58 alloy increases the rate of the G P B to S precipitate transformation since there is a high dislocation density in which the S precipitate nucleates.

Fe and Ni additions have significant effects on the age hardening of the alloy when they exist separately because the separate compounds take up some of the copper that would be otherwise available for hardening, but the combined $FeNiAl_9$ compound that forms when both are present takes up to only 1% Cu.[2]

2.4 S' Phase

Silcock[1] and Bagaryatski[6] examining Cu : Mg of 2.2 : 1 ratio found that G P B zones are formed in the early stages of ageing at 190°C and followed by nucleation of S' lath like platelets and their growth as laths on $\{210\}$ matrix planes with the relationship to the aluminium matrix:

$$100_S \,//\, 100_{Al} \;:\; 010_S \,//\, 021_{Al} \;:\; 001_S \,//\, 012_{Al}$$

The long axis of the lath $[100_S]$ lies along the cube edge in the matrix lattice with the large face of the lath lying on a $\{210\}_{Al}$ plane. Several $\{210\}_{Al}$ planes are normally utilised by the laths growing from any given dislocation so developing composite precipitate sheets.

Wilson and Partridge[12] examined the nucleation and growth of S' precipitates in a 2.5% Cu 1.2% Mg alloy. They reported that sheets of S' precipitates can be formed on dislocations by laths lying on the $\{210\}$ planes having common $\langle 100 \rangle$ growth direction.

They suggested that since the formation of the S' precipitate is by heterogeneous nucleation at dislocations, then increasing the dislocation density by pre-strain prior to ageing would be one method of refining the S' precipitate distribution. Since there would be an increase in the number of nucleating sites for a given solute content, then the final precipitates would be smaller.

This has since been observed by Wilson & Forsyth[2] who referred to the work of Vaughan[13]. Hardness reaches a maximum when approximately 25% of the S' phase has formed and a large proportion of G P B zones still remain. Further ageing corresponds with the re-solution of G P B zones and the growth of S' platelets with the final transformation of S'

to S. This represents an overageing of the alloy and is accompanied by softening.

Wilson, Moore and Forsyth[11] examining the effect of silicon on precipitation in a 2.5% Cu 1.2% Mg alloy reported that a 0.25% Si addition modified the as-quenched defect distribution by reducing the number and size of the vacancy loops and dislocation helices. This altered the distribution of S' precipitate.

While heterogeneous precipitation still occurred, a more uniform precipitate was noted and the density of precipitates was increased suggesting either homogeneous nucleation or heterogeneous nucleation at sub-microscopic sites.

The nucleation of S' precipitates was retarded and their growth rate was reduced by the presence of silicon, but their average length after long ageing was little affected.

The refinement of the intermediate precipitate S' by the addition of silicon was probably a direct consequence of its influence upon the formation of G P B zones. Silicon decreases the rate of formation of G P B zones, but the coherency strain associated with their formation was increased, resulting in increased hardening.

Brook and Parsons[14] have observed that silver, like silicon, increased the hardness of an Al-Cu-Mg alloy due to G P B zone formation. Although silver was not present in the test alloy, reference to silver is included here as comments on possible benefits to be obtained by the addition of silver to the test alloy are made in the conclusions.

Sen and West[15] found that the addition of silver produced a marked increase in proof stress and an increase in the density of the S' precipitates.

A cuboid precipitate detected by Weatherley and Nicholson[16] was

found to be formed concurrently with the S' precipitates in the silicon alloys and this was possibly Mg_2Si or silicon. The S' precipitates are a semi-coherent form of the S phase. They are coherent with the matrix on $\{210\}$ planes and are lath like precipitates of Al_2CuMg.

The properties of a dislocation may change after it has acted as a nucleating site for precipitates. Kelly and Nicholson[18] suggest that if the precipitate is partially coherent the dislocation becomes a structural dislocation at the precipitate-matrix interface. It is thus part of the precipitate and cannot be torn free during plastic deformation although possibly lengths of dislocation line between precipitates might act as Frank-Read sources under high stress. If the precipitate is non-coherent (S phase) a single dislocation line absorbs such a small proportion of the misfit at the interface that it seems possible that it could be torn away during plastic deformation. Other observations relating to the effects of pre-strain on creep strength also suggest that there is no strong bonding between the precipitate and the dislocation.

2.5 S Phase

This has the same composition as the S' phase but is non-coherent with the lattice.

It was shown by Perlitz and Westgren[19] to have the composition Al_2CuMg and to be face centred orthorhombic with a = 4.00, b = 0.23 and c = 7.14 A^{o}. As ageing time increases the G P B zones disappear and growth of S' and its transformation to S precipitate occurs in the matrix leading to softening. Heterogeneous and rapid formation of S' and S on grain boundaries and dislocations can occur simultaneously with the slower ageing process in the bulk of the matrix.

2.6 Intermetallic Particles

The phases present in RR 58 (the French equivalent made under licence is AU2GN) have been examined by Moulins and Adenis.[20]

In the as-cast alloy particles of $FeNiAl_9$, Mg_2Si and $Al_4CuMg_5Si_4$ are present. On homogenising at 525°C (470°C used in this test alloy) there is mainly $FeNiAl_9$ and Cu_3NiAl_6 with the silicon bearing phase entering into solution. After solution treatment there is mainly $FeNiAl_9$ with some Cu_3NiAl_6 and only traces of others. This remains after ageing.[20]

The particles of $FeNiAl_9$ vary between 1 and 10 μm in diameter and are usually randomly distributed except when subjected to prior mechanical working which often results in the particles forming layers. Although there is some increase in tensile strength there is little or no apparent effect upon the precipitation hardening process, but the particles do appear to stabilise the grain size.

2.7 Hardness

It is generally accepted that the behaviour pattern of RR58 alloy follows that suggested by Silcock for an Al:Cu:Mg alloy (2.2 Cu 1.0 Mg):-

Ageing sequence

At 30°C G P B only

At 110-190°C G P B → G P B + diffraction streaks without change of hardness

→ G P B + S' (the highest hardness obtained when about 25% of the S' has formed and a great deal of G P B remains)

→ S' (G P B decreases and S' increases as the hardness decreases)

→ S (final decrease in hardness).

Figure 2 shows the properties of various alloys including an RR58 of Al 2.5Cu 1.2Mg 1.0Ni 1.0Fe 0.25Si and there was little variation between 12 and 24 hours. For 0.66 day ageing time a VHN of about 140 was obtained. The Fe + Ni alloy had higher hardness than one with just Fe or Ni but all contained Si. All alloys containing Si were harder than those without Si. The RR58 used for the present tests contained low Si.

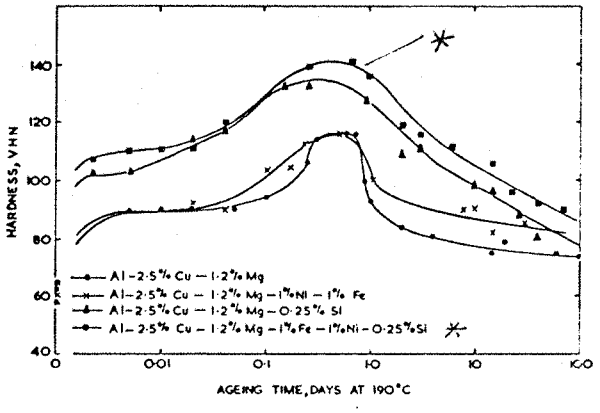

Effect of 0·25% silicon on the age-hardening at 190° C of an Al-2·5%Cu-1·2%Mg and an Al-2·5%Cu-1·2%Mg-1%Fe-1%Ni alloy. (Ref.2)

FIG.2

Silcock found a hardness of 140 at peak for Al 3.15Cu 1.52Mg aged at 190°C for about 19 hours.

Forsyth, Wilson & Moore[11] suggest that a higher density of smaller S' precipitates in the alloy were produced by the addition of silicon but that much of the hardness must have been the result of the improved strength of the G P B zones.

The alloy used in the present work had 1.88Cu instead of 2.5 and

Mg 1.74 instead of 1.2 but both alloys are within the RR58 composition range. The results are similar to reported values; 130 VHN in present tests compared with 138-140 for similar compositions as given below.

A peak hardness of 138 VHN for RR58 aged 30 hours at 190°C was reported by Dewey.[21] A peak hardness of 142 VHN after ageing 11 hours at 190°C was found by Hardy[22] for an alloy with Cu:Mg ration of 2.2:1.

Many workers have reported that cold working an aluminium alloy brought about general precipitation more rapidly.[23] Gayler reported that cold rolling and then ageing at 200°C reduced the time to reach peak hardness from 8 hours to 55 minutes. Gayler also found that the rate of quenching of an Al-4%Cu alloy influenced the hardness and interrupted quenching is now well known to vary precipitation behaviour in a number of alloys.[24]

In the present tests a check on ageing hardness was carried out on the $\frac{1}{4}$ cycle material (unidirectional stretch) at 190°C over a time scale of 13 hours to 72 hours. Very little variation was found in the VHN. This suggests that the major change in hardness with ageing time occurred at less than 13 hours, and that in keeping with the findings of Gayler on a different alloy there had been a considerable reduction in the time to reach plateau hardness.

Application of the 19 hours ageing time in the present test material suggests that the $\frac{1}{4}$ cycle, 3 cycle and 1000 cycle material were all fully aged. The susceptibility of subsequent precipitation to quench rates, stepped quenching and time held at room temperature for the pre-straining together with the influence of additions of varying amounts of Si and Cu makes prediction of a general pattern of hardness behaviour complex. Very careful control of these aspects is necessary and more investigation necessary to determine the interaction of variables.

2.8 The Role of Vacancies

A vacancy is an atom site unoccupied by an atom. A number of vacancies may condense in one zone to form a pore or sheets of vacancies may collapse to form sessile dislocation loops.

Vacancies are closely connected with diffusion processes i.e. the movement of atoms from one lattice site to another. Diffusion is important in such processes as homogenising, annealing and recrystallisation, phase changes and precipitation processes in age hardening.

Work using radio-isotopes has confirmed that diffusion of substitution atoms involves vacant sites and that diffusion of vacancies in one direction is accompanied by diffusion of atoms in the opposite direction. Increasing the number of vacancies in an alloy increases the diffusion rate.

Diffusion rates may be increased by (1) Temperature increase, (2) Cold work. An increase in temperature increases the number of vacancies and quenching rapidly from a high temperature retains large numbers of vacancies thus creating a vacancy supersaturation compared to a slowly cooled alloy.[25,26,27]

The excess vacancy concentration accelerates the subsequent metallurgical processes such as precipitation hardening. Cold working of an alloy introduces more imperfections into the lattice and diffusion rates are raised, although the increase may be due mainly to the imperfections acting as sinks. The rate of quenching, stopping the quench at an intermediate temperature and then continuing the quench have important influences on the subsequent behaviour of an alloy.[28]

The supersaturation of quenched in vacancies is locally reduced by diffusion to sinks, such as grain boundaries, free surfaces, dislocations or by clustering together of vacant sites to form dislocation defects as

described earlier. In dilute aluminium alloys (Al - Cu) vacancies tend to cluster together on close packed planes and then collapse to form dislocation loops.[4]

Structural instability can be introduced by a high concentration of vacancies and Broom[29] has considered many possibilities:-

(1) The moving of dislocations may create vacant lattice sites and thereby increase the diffusion rate. This results in localised overageing comparable with isothermal behaviour at higher ageing temperatures.

(2) Multiplication of dislocations and an associated increase in diffusion rate can lead to increased possibilities of "short circuit" diffusion paths (pipe diffusion).

(3) Mobile dislocations may interact with sessile dislocations forming the boundaries of coherent precipitates causing the precipitates to become non-coherent with subsequent reduction in local elastic strain.

(4) The nucleation of stable precipitates may occur which is a process of overageing. The S phase is the stable precipitate in the test alloy, the S' stage being meta-stable.

(5) Within slip bands the moving dislocations may generate sufficiently high temperatures for normal ageing to take place leading to softening and cracking, although there is some doubt about the temperature that may be achieved by this mechanism.

(6) It has been suggested that dislocations may drag solute atoms from precipitate, thereby causing resolution.

CHAPTER 3

FATIGUE

3.1 Introduction

Engineering components fail under repeated loading and unloading or under reversal of stress, often at stresses smaller than the ultimate strength of the material of the component under static loads. The magnitude of the stress required to produce failure decreases as the number of cycles of stress increases. This phenomenon of the decreased resistance of a material to repeated stresses is called fatigue. Fatigue is a complex phenomenon, involving both microscopic flow processes and macroscopic crack extension.

A vast amount of research and investigation has been carried out, the earlier work consisting of the accumulation of fatigue test results for particular materials and components and the use of these to construct diagrams for the prediction of performance.

Microscopic examination of specimens began just after 1900 and were concerned with iron.[30] Fatigue became an increasing problem with the advent of higher speed travel, the need to reduce weight of components, new materials and environments. These investigations are broadly divisible into the following:-

(a) Testing of full size components or structures.

(b) Testing of standard plain or notched specimens to establish data for comparison and prediction.

(c) The crack initiation process.

(d) The crack propagation process.

(e) The formation of rules relating to cumulating damage and more empirical work establishing the crack initiation period and the subsequent crack propagation rate.

There is difficulty in relating the test results on standard plain or notched specimens to the performance of the material in an engineering component or structure. This is in part due to the many variables which influence the service result in practice, although it is clearly desirable that the fatigue data used for design shall have been produced under conditions similar to those anticipated in practice. The value of tests on standard plain or notched specimens is that the effects of various influences may be examined and the knowledge is of value in selecting materials for particular practical situations. There is also a problem related to the chance occurrence of defects and therefore a basic size effect may appear.

Variables which effect test results include:-

(a) Engineering surface condition.

(b) High stress levels that introduce special effects.

(c) Temperature.

(d) Environment.

(e) Shape and size of specimen and type of test (stress gradients).

Other variables, some related to microstructure or material quality which effect the test results are:-

(f) Prior load history. Cold work.

(g) Grain size.

(h) Second phase instability. The appearance of metallurgical flaws or defects may increase the scatter in fatigue results.

The above are extensively reviewed in the literature[31-43].

There was considerable emphasis on the crack initiation process at one time but interest then shifted to the crack growth processes. Particularly in the aircraft industry with the advent of fail-safe design philosophy.

Improvements in the fatigue resistance to crack initiation have been made by the use of such techniques as shot peening, nitriding and carburizing. There are however many situations in which the overriding weakness is a point of stress concentration such as a notch or hole, or fretting occurs. In such circumstances the crack initiation stage is overwhelmed by the crack growth stage and 'fail safe' techniques are evolved based on the acceptance of a cracked engineering component in service conditions, and its removal from service when the crack has reached a certain length.

Fatigue may be represented by a number of stages which may involve different mechanisms. Models of such stages were proposed by Forsyth and Ryder[44] and extended by Forsyth[45] and their terminology has been common in the literature since that time.[31]

3.2 Crack Initiation

Fatigue crack initiation in smooth specimens of ductile crystalline materials often occurs in slip bands. Forsyth[46,47] had observed the slip band extrusion effect, and Cottrell and Hull[48] and Forsyth[49] had discovered the inverse process, slip band intrusion. Cyclic straining produces changes in the surface by the formation of slip bands. Some slip bands become persistent which cannot be removed by annealing. Intrusions may form from a slip band groove and extrusions may develop from a ridge. (Fig. 3). Slip bands produced by unidirectional stress are usually surface steps, while fatigue bands may be either grooves or ridges having 'saw tooth' form. (Figs. 4 and 5).

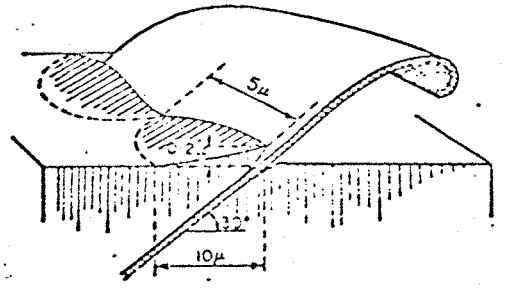

(a)

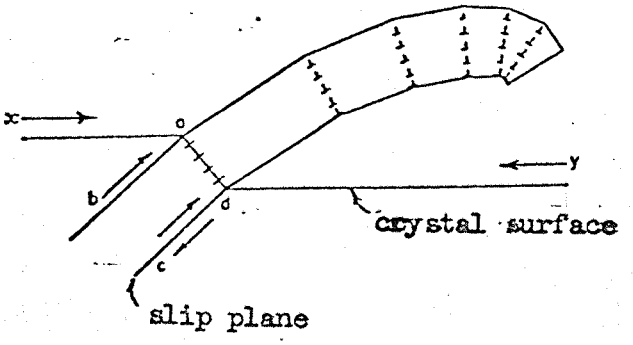

(b)

FIGURE 5 EXTRUSION

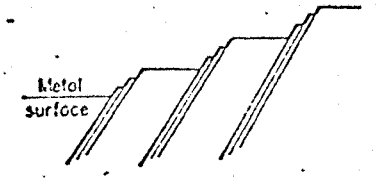

Steady Stress

FIGURE 4

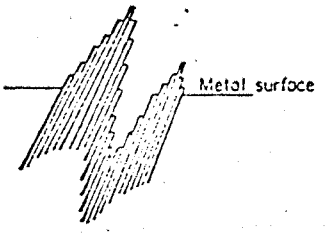

Cyclic Stress

FIGURE 5

SLIP IN METALS

Slip bands associated with holes were found by Forsyth to form in age hardened aluminium 7.5%Zn 2.5%Mg alloy. Subsequent solution treatment eliminated the persistent slip zones but failed to heal the holes.[50]

When crack initiation starts at a surface it has been found that the specimen may be returned to its original condition of life by machining off the crack. It has been found possible to repeat this process time and time again on the same specimen. Slip band intensification occurs in grains favourably orientated to the maximum shear stress and at a free surface the intrusions finally develop into cracks along the shear bands.

In age hardened alloys localised resolution or precipitate over-ageing may occur.[51] There may be changes such as polygonisation, recrystallisation, changes in mechanical properties and lattice defect concentration.[52]

Cross slip occurs readily in aluminium alloys and it has been reported that for another material[53] in which cross slip occurred easily the crack initiation was at the grain boundary. This weakness of the grain boundaries is occasionally observed in a variety of alloys.

3.3 Stage I Crack Growth

The initial crack may deepen on a plane or planes of high shear stress. Stage I may be absent in highly stressed specimens but in low stressed specimens may represent 90% of the life. Transgranular, intergranular and mixed mode Stage I cracks have been reported in aluminium alloys (Forsyth et al [54,55]). Stage I cracks, associated with local bands of substructure produced by loading, have also been noted by Forsyth but the way in which the sub-structure is associated with the

crack is not clear. The large amount of plastic deformation associated with the crack tip is thought to account for the substructure cell formation.

The Stage I initiation and early growth in precipitation hardened aluminium alloy is clearly associated with some precipitate destruction along slip planes. Stage I fractures are often featureless except for damage arising from the rubbing of mating surfaces. Figs. 6 and 7 are representative models of the processes.

Stage II Crack Growth

Following Stage I which was associated with shear stress there arises Stage II cracking producing a general surface normal to the principal tensile stress. This generally forms the largest part of the fracture surface although the crack growth period in this mode possibly represents not more than 10% of the total life for a smooth ductile specimen.

The characteristic markings of fatigue failure known as striations may occur in this stage. They are more pronounced in some materials e.g. aluminium alloys, than in others such as steels. Striations were observed in the electron microscope in the present work are shown in Plates 1 to 6. Striations are commonly classified into ductile and brittle striations. These are illustrated in Figs. 8 and 9.

Type A are ductile striations which have the form of ridges lying on irregular non-crystalline plateaux, generally orientated normal to the principal tensile stress.

Type B are brittle striations lying on crystallographic facets. They are joined by regions of ductile tearing which appear as steep cliffs which often exhibit a fan-like appearance.

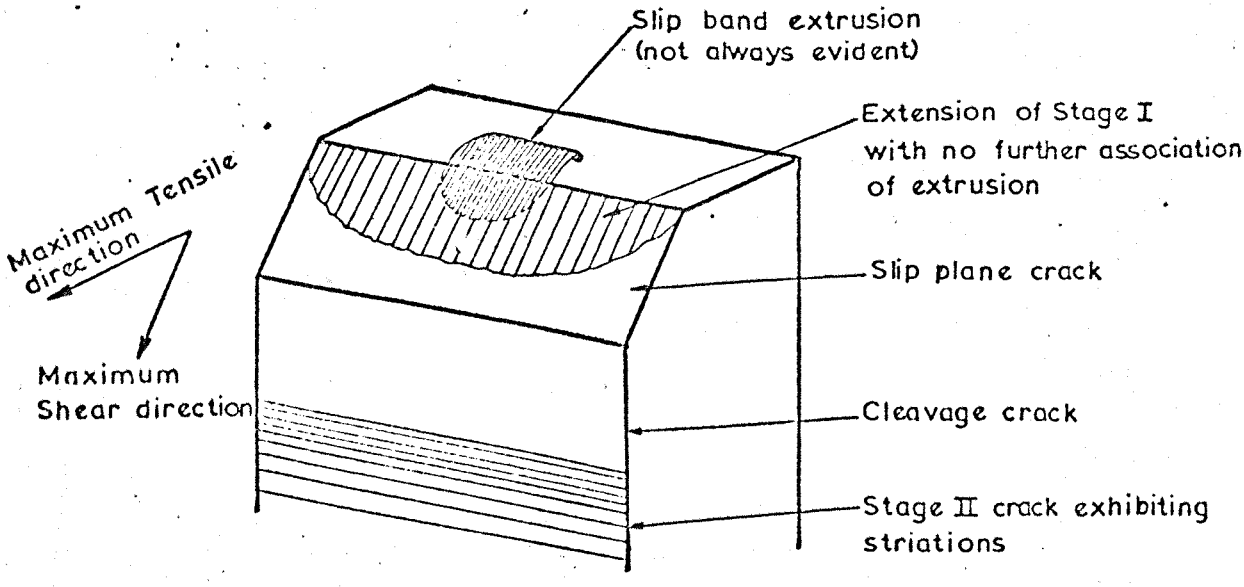

FIG. 6 DIRECT STRESS FATIGUE CRACK GROWTH (Forsyth, Ref. 45)

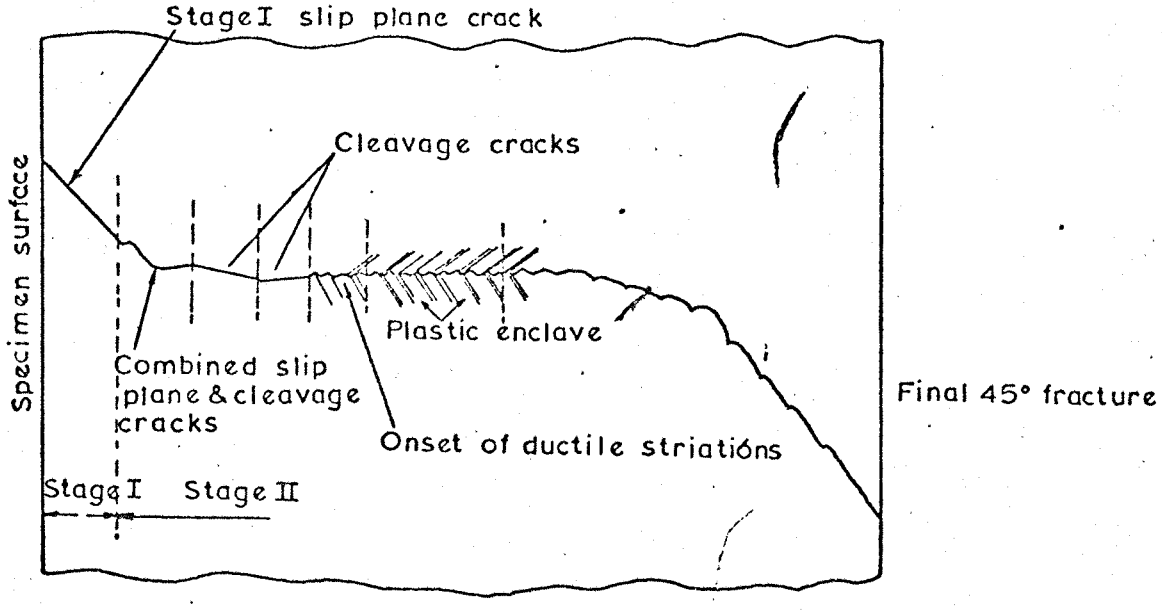

FIG. 7 SCHEMATIC ILLUSTRATION OF MODES OF FATIGUE FRACTURE IN STRONG ALUMINIUM ALLOYS (REF. 45)

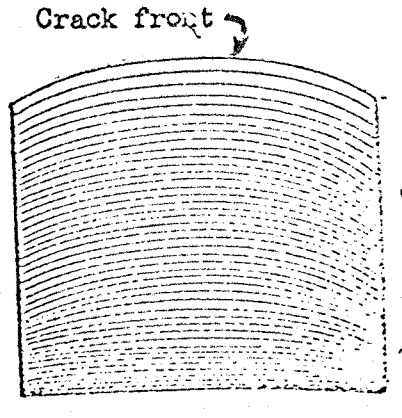

FIGURE 8

(a) DUCTILE FRACTURE STRIATIONS

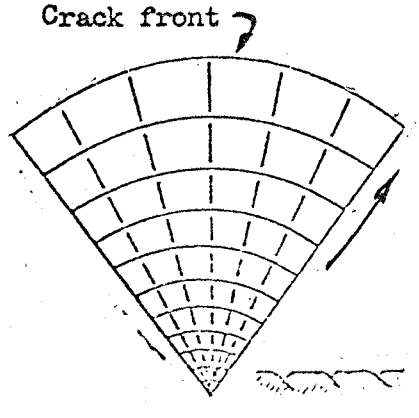

FIGURE 9

BRITTLE FRACTURE STRIATIONS

FIGS. 8 & 9 SCHEMATIC DIAGRAMS INDICATING STRIATIONS (Ref.45)

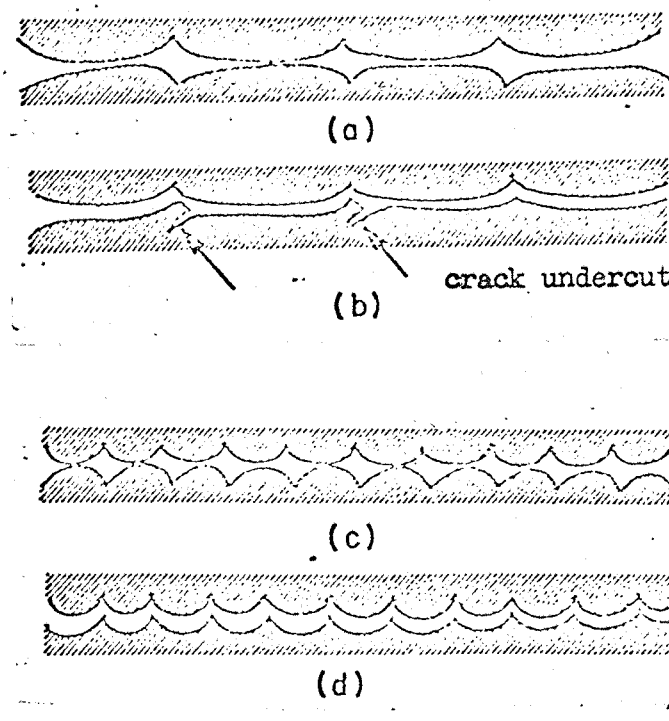

(a) and (b)

AT HIGHER STRESSES

(c) and (d)

AT LOWER STRESSES

FIG.10 VARIOUS TYPES OF MORPHOLOGY EXHIBITED BY STRIATIONS ON DUCTILE FATIGUE FRACTURE SURFACES, VIEWED IN PROFILE. THE STRESS AXIS IS VERTICAL. (Ref.35)

Several forms of striation have been observed[56] and these are shown in Fig. 10.

(a) and (b) are the type produced in ductile metals and alloys at high stresses.

(c) and (d) are the type produced at lower stresses in the same materials.

Stubbington showed the existence of saw-tooth striations in which the peaks of one fracture surface coincide with valleys on the matching fracture surface. He considered one wall of the striation to be produced by brittle cleavage but the other by plastic flow.

A number of mechanisms have been proposed to account for the profiles and the characteristics of crack propagation. These include those of (1) Forsyth & Ryder[57] in which a void ahead of the main crack joins up to it by void coalescence. (Fig. 11). (2) The 'Plastic Blunting' mechanism as described by Laird[56] and shown in Fig. 12. Hertzberg[58] proposed an intersecting slip mechanism to explain why striations may be absent or minor. The problem of microcrack propagation has been discussed in terms of dislocation flow and fracture mechanics but no universal connecting law has been evolved.[33]

There has been emphasis on the use of the stress-intensity factor for the correlation of data for widely varying combinations of loading and crack geometries. This approach has not proved satisfactory at high cyclic stresses due to the influence of plasticity and fracture instability.

There are many cases in which cracks nucleate at specific sites but not necessarily going through the classic model of Stage I crevice formation. These include[31]:-

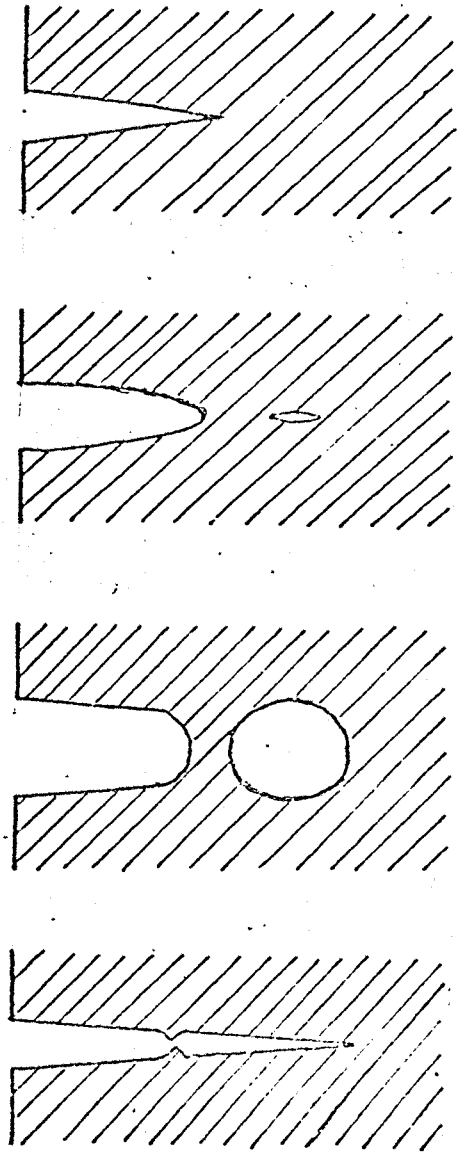

(a) OPENING OF CRACK UNDER TENSILE STRESS

(b) PLASTIC BLUNTING OF CRACK TIP AND FRACTURE AHEAD OF MAIN CRACK

(c) COALESCENCE OF THE ADVANCE VOID WITH MAIN CRACK BY DUCTILE NECKING

(d) COMPRESSION RE-SHARPENS CRACK

FIGURE 11 A mechanism of fatigue crack propagation involving true fracture ahead of the crack tip (Ref.44)

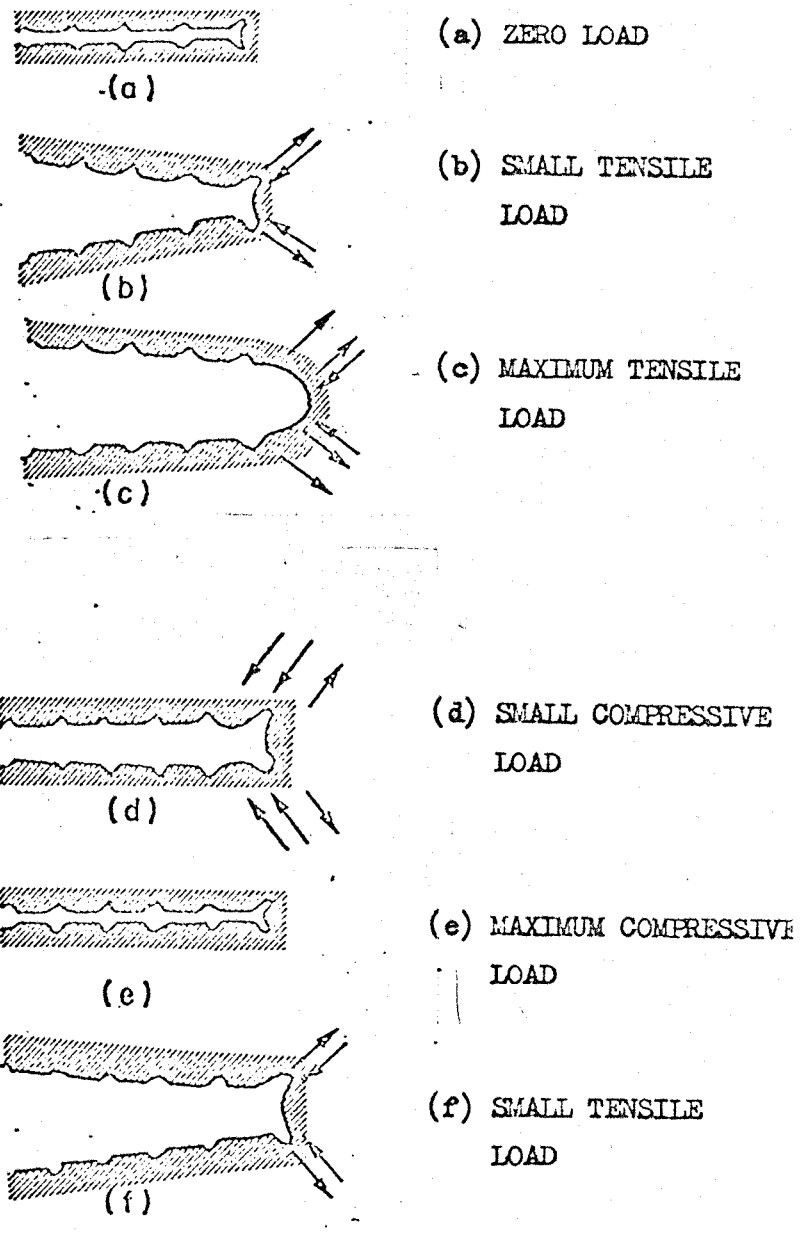

FIGURE 12 The plastic blunting process of fatigue crack propagation in the Stage 2 mode(Ref.35)

The double arrowheads in (c) and (d) signify the greater width of slip bands at the crack in these stages of the process. The stress axis is vertical.

(a) In alloys, particles of second phase,[59] especially if fragmented by prior mechanical working, can initiate cracks, as may weak particle/matrix interfaces.

(b) Grain boundaries.[60,61]

(c) Annealing-twin/matrix interfaces in f.c.c. metals.[60-63]

(d) Twin/matrix interfaces[64-67] and fragmented deformation twins in other crystal structures.

(e) Sharp corners, machining marks etc. in components often promote the initial crack.

3.4 Fatigue in Aluminium Alloys

Precipitate hardened alloys of aluminium do not have good fatigue properties and their fatigue strength/tensile strength ratio is normally in the range 0.2 to 0.3.

Much of the weakness in fatigue has been attributed to the presence of large inclusions[59] but fatigue induced precipitate free zones or precipitate depleted zones must play an important part in this special fatigue weakness.[68,69] It has been found that precipitate free zones adjacent to grain boundaries provided a region of easy crack initiation and growth and also that large boundary particles produced by overageing[70] started intergranular fracture.

There is a tendency for a continuous cellular structure to be formed if the cyclic strain is large or if the alloy has a high stacking fault energy. This is due to increased tendency for cross slip. Ease of cross slip, stacking fault energy, work hardening and substructure are related variables. Sub-structure and the association of fatigue with a type of substructure have been reported by many workers.[71-73] Grosskreutz and

Waldow[72] examined the substructure and fatigue fracture in aluminium and found at low strain amplitudes ($\epsilon = 3 \times 10^{-4}$) both subgrains and loop patches depending upon the orientation of a particular grain. In a high stacking fault energy material like aluminium some subgrain formation always exists at the tip of a fatigue crack.

Propagation of the crack occurs along the subgrain boundary because the higher energy of this region will lower the total work necessary to fracture. The other choice with which the crack is presented is to propagate through the matrix along slip planes. Such slip plane cleavage was not observed in the experimental results of Chin, Backofen and Grosskreutz[74,75] who worked with bi-crystals and single crystals of aluminium. At low cyclic strain amplitudes the type of substructure formed was found to vary from grain to grain[72] and must therefore be a function of the orientation of the grain with respect to the tensile axis. Because the formation of sub-boundaries along low crystallographic planes requires the interaction of dislocations on more than one slip system, it follows that those grains orientated for multiple slip are most likely to form sub-grain structures first, and, therefore, the substructure distribution may be heterogeneous.

CHAPTER 4

DEVELOPMENT OF TEST APPARATUS

Slow Cycling Attachment to Losenhausen UHP 60 Machine

The existing Losenhausen UHP 60 testing machine was converted into a slow cycling machine by devising a pumping circuit to supply the existing tensile piston and a new compression piston alternately. The tensile piston is shown at A in Fig. 13 and the compression piston cylinder was fitted into space B. The compression cylinder is omitted from the set up for clarity. The attachment gave alternating loads up to 600 kN tension and 300 kN compression. Figure 14 shows the layout of the pumping circuit. The system is supplied by the pump from the static control panel through two solenoid valves (3 and 4), which are in turn operated by pressure switches (1 and 2) when the set hydraulic pressure is reached.

The tension load is measured on the pendulum gauge P_o (existing) and the compression load on the small manometer gauge P_u which was added. Throttle valves (5 and 6) are used to restrict the flow in the exhaust line so altering the wave shape. Two shut off valves are provided to protect the gauges when the machine is cycling. The cycling range could be varied between 50 kN compression to 600 kN tension, the cycling speed depending upon the range chosen but of the order 10 to 60 Hz.

The attachment was found to be simple to operate but one difficulty was encountered; the construction inside the cross head above piston B was unknown and Losenhausen stated that this was capable of taking compression. It was found that this was not the case and a bridging piece had to be manufactured in the workshops to bridge the lower end of piston A and transmit compression forces to the main cross head above piston B.

The machine as adapted was suitable for the purpose of applying cyclic pre-strain to large bulk specimens of RR58 alloy. The speed of cycling was limited by the use of the existing pump to alternately supply the tension and compression pistons. This was done because of cost but the introduction of a separate pump to supply the compression piston would increase the cycling speed.

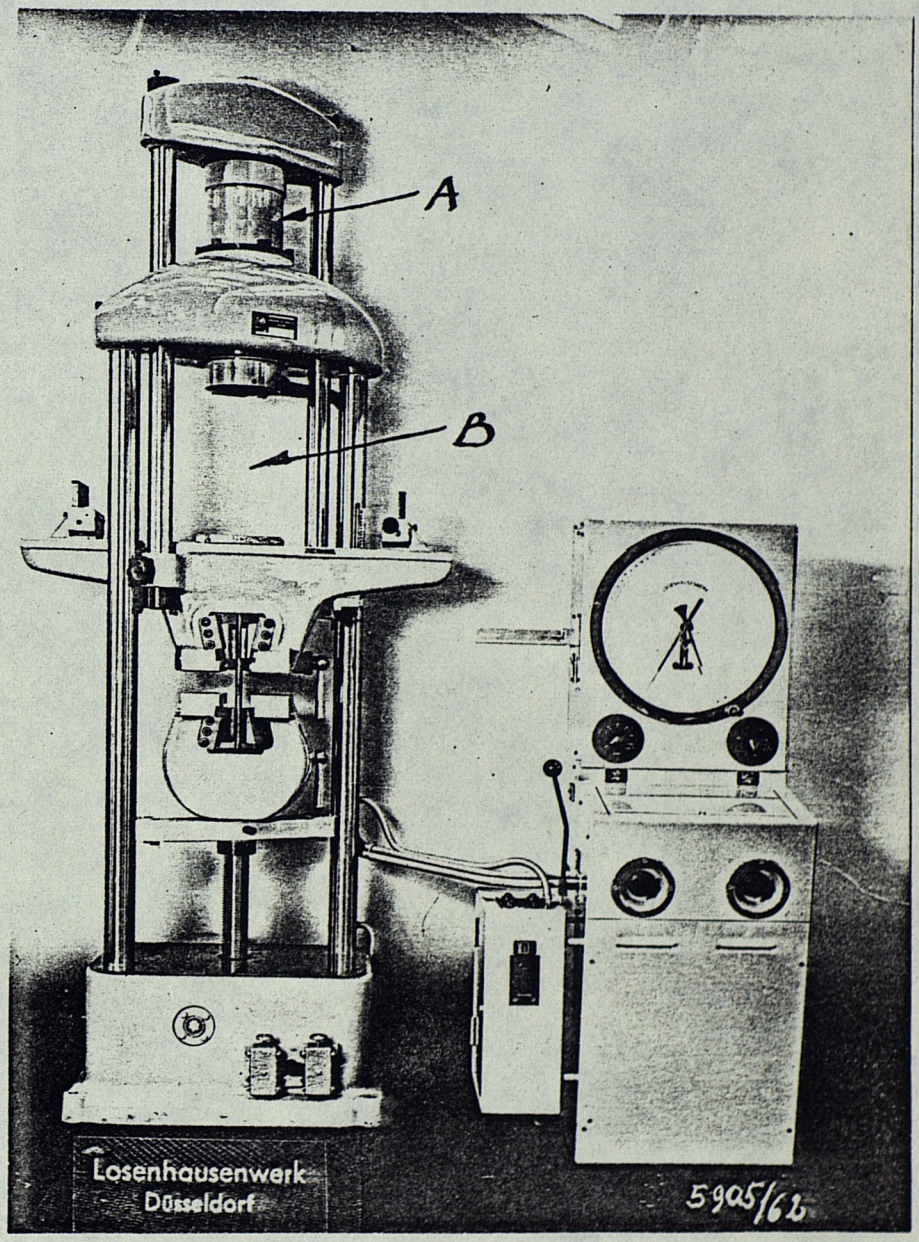

FIG.13 LOSENHAUSEN UHP 60 MACHINE

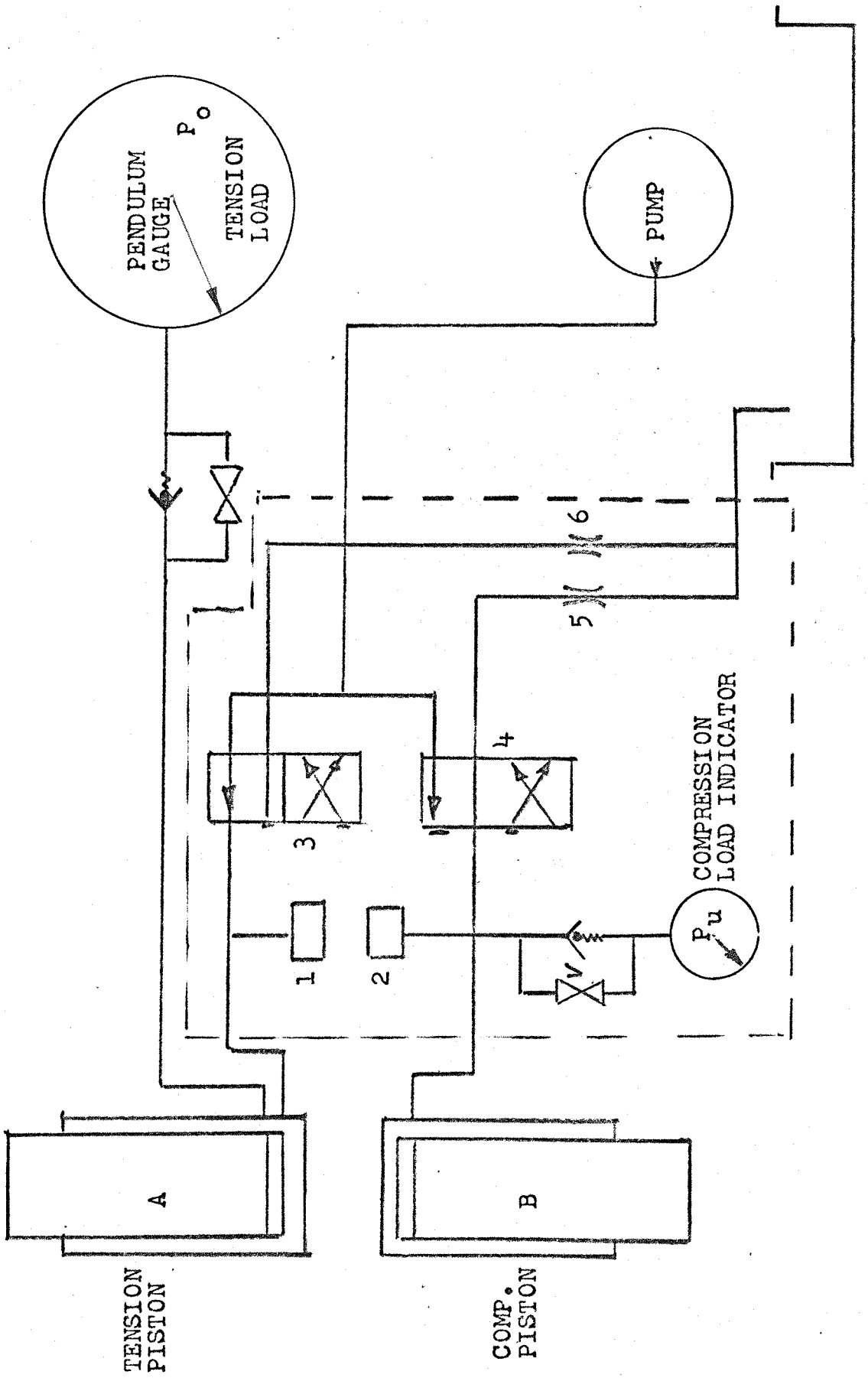

FIG. 14 CIRCUIT FOR CONVERSION OF LOSENHAUSEN UHP 60

CHAPTER 5

MATERIAL PREPARATION

5.1 RR58 Alloy (see Table 1 for composition comparison)

Test alloy composition:-

Cu 1.88 Mg 1.74 Ni 1.12 Fe 0.99 Si 0.14

The test alloy was degassed and grain refined and then water chill cast in 150 mm (6") diameter ingots using mains water. It was then homogenised at 470°C for 16 hours. The ingot was machined to remove the surface irregularities, forged and hot rolled into plates of 16 mm ($\frac{5}{8}$") thickness and 275 mm (11") width.

5.2 Cutting, Pre-strain and Ageing Details

The plate was cut into large specimens which were pre-strained in the solution treated condition in the following manner:-

Specimen 1 Unidirectional stretch ($\frac{1}{4}$ cycle)
Tensile only to 266 MN/m^2 (17 ton/in^2)

Specimen 2 3 cycles ($3\frac{1}{2}$ performed as necessary to unload from the tension side)
Stress plus or minus 266 MN/m^2 (R = -1)

Specimen 3 1000 cycles
Stress plus or minus 266 MN/m^2 (R = -1)

Specimen 4 No pre-strain (Zero cycle)

The large specimens used for pre-straining in the solution treated condition were sawn from the rolled plate and were approximately 297 mm x 59 mm x 16 mm for the 3 and 1000 cycle specimens.

Cycling pre-strain was carried out in a Losenhausen UHP 60 testing machine of capacity 600 KN (60 ton) which had been specially converted for the purpose by adding an additional ram and a cycling control mechanism. A diagram of the circuit and photograph of the Losenhausen as converted is included. (Figs. 13 and 14).

In the commercial use of RR58, refrigeration or a stabilising treatment have been used to restrict ageing of the material at room temperature prior to its artificial ageing. The stabilising of the commercial alloy consists of heat treatment at 150°C for a short time after solution treatment.

The test alloy was not stabilised as it was thought that this would add an additional complexity to the variables influencing the test results. The test alloy was kept in a refrigerator whenever possible but the 1000 cycle pre-strain of specimen 3 was carried out over a period of 25 hours at a room temperature of 16 to 17°C at 40 cycles per hour and natural precipitation during deformation cannot be ruled out.

Any specified pre-strain of the large specimens was followed by artificial ageing treatment consisting of 19½ hours at 190°C.

5.3 After Pre-strain and Ageing

The large specimens were then sawn into small rectangular blocks as shown in the cutting diagrams Figs. 15 to 18 from which Rolls-Royce-Type fatigue specimens were machined. The fatigue specimens were marked in blue at the end facing the anchor block and the longitudinal axes of specimens lay along the length of the plate and parallel to any pre-strain force. The pattern of the test pieces in each large specimen was recorded to check possible variations due to the position of the fatigue specimen in the large specimen.

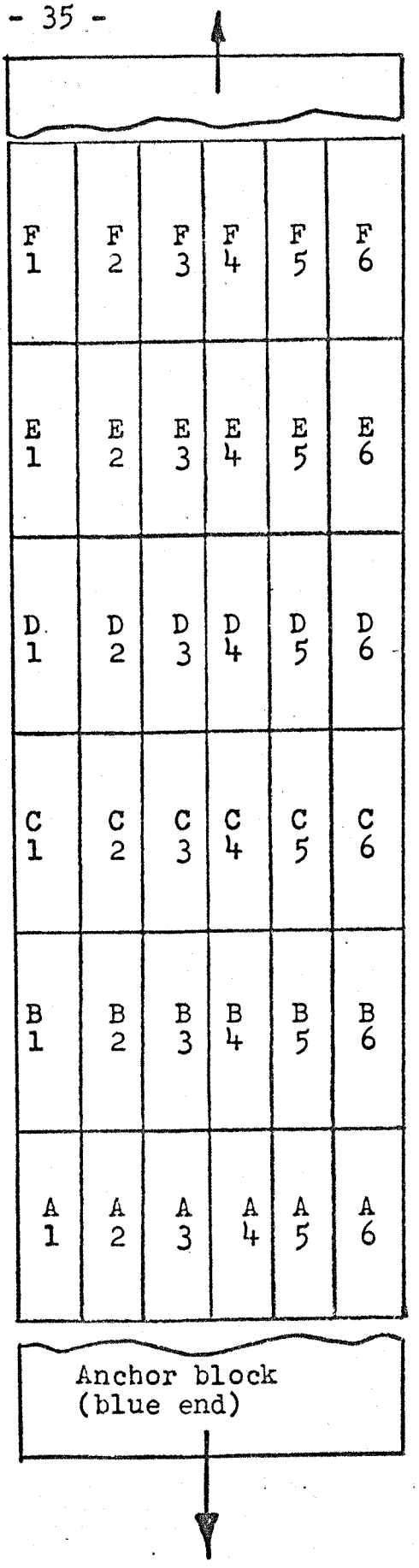

FIG.15 POSITION OF ¼ CYCLE (UNIDIRECTIONAL STRETCH) ROLLS-ROYCE-TYPE FATIGUE SPECIMENS.

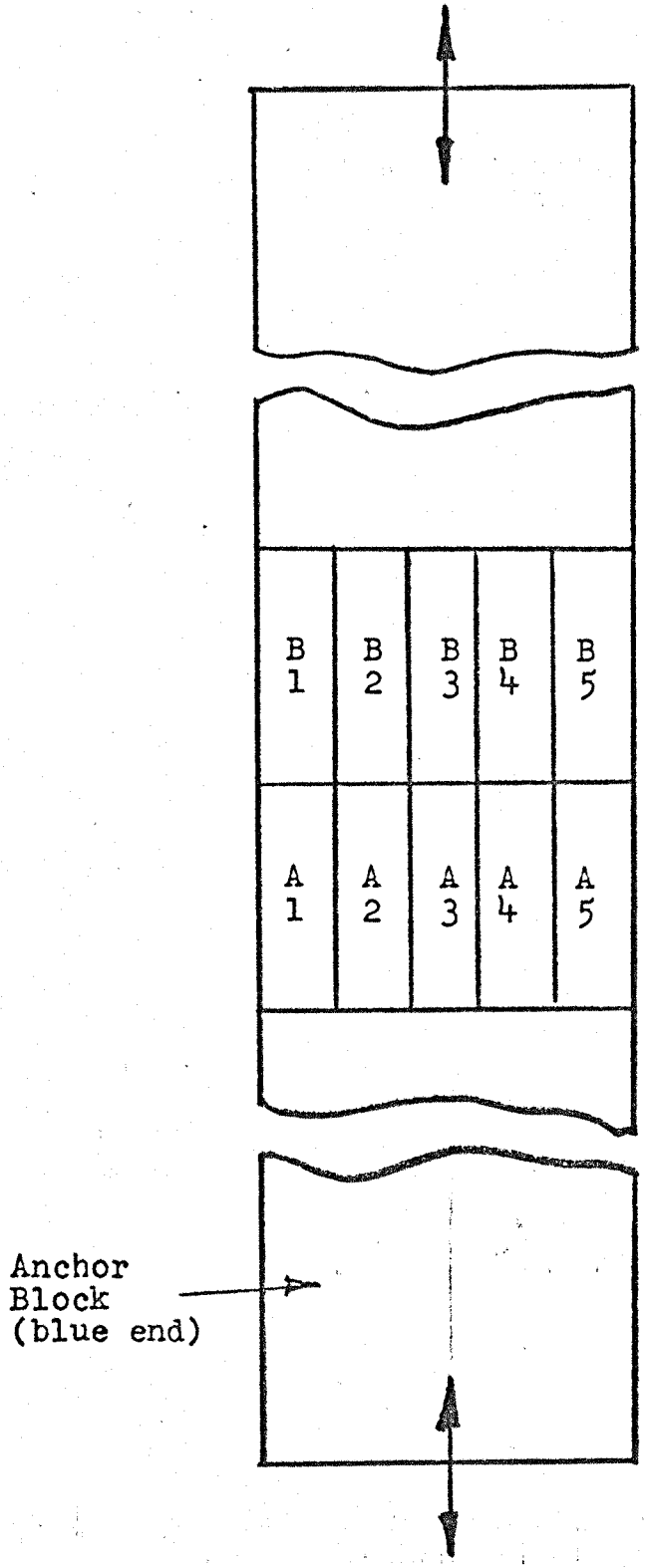

FIG. 16 POSITION OF 3 CYCLE PRESTRAIN ROLLS-ROYCE-TYPE FATIGUE SPECIMENS.

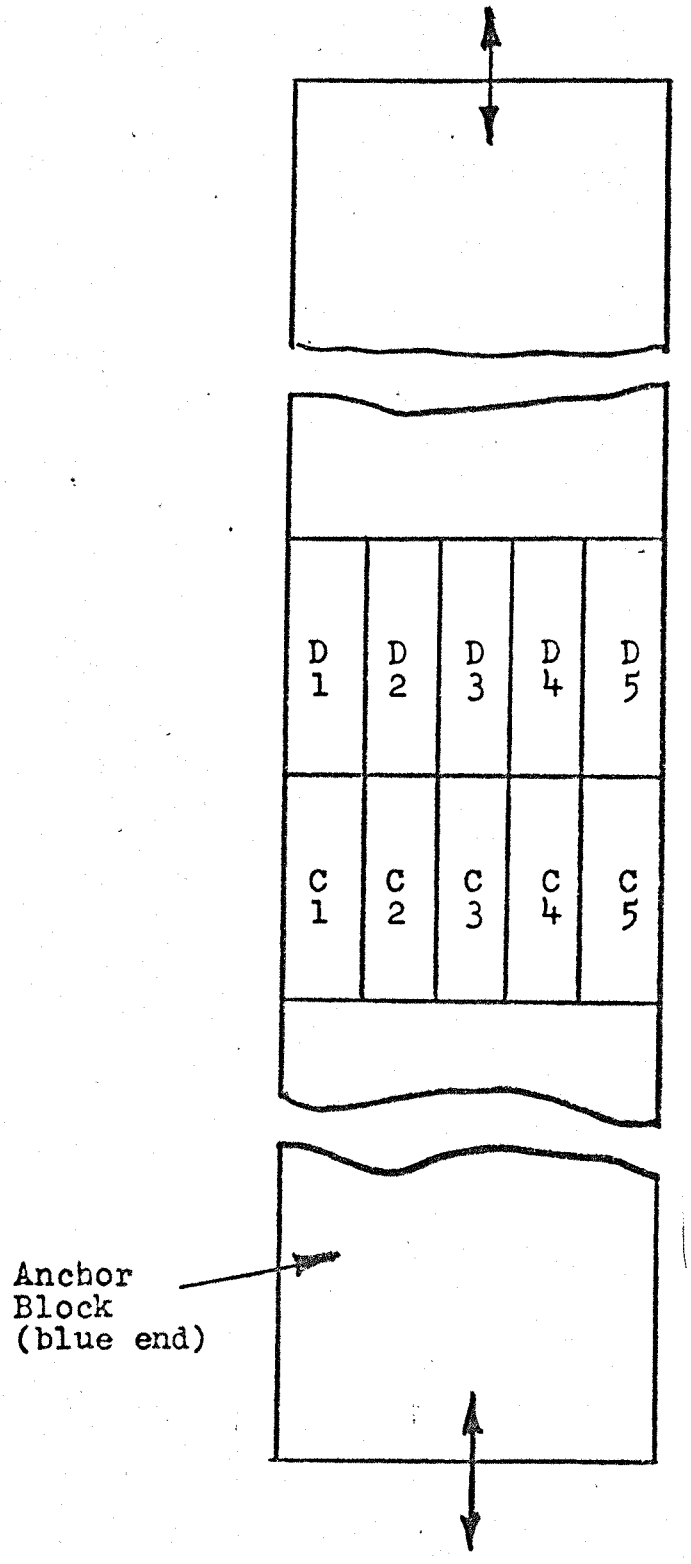

FIG. 17 POSITION OF 1000 CYCLE PRESTRAIN ROLLS - ROYCE - TYPE FATIGUE SPECIMENS.

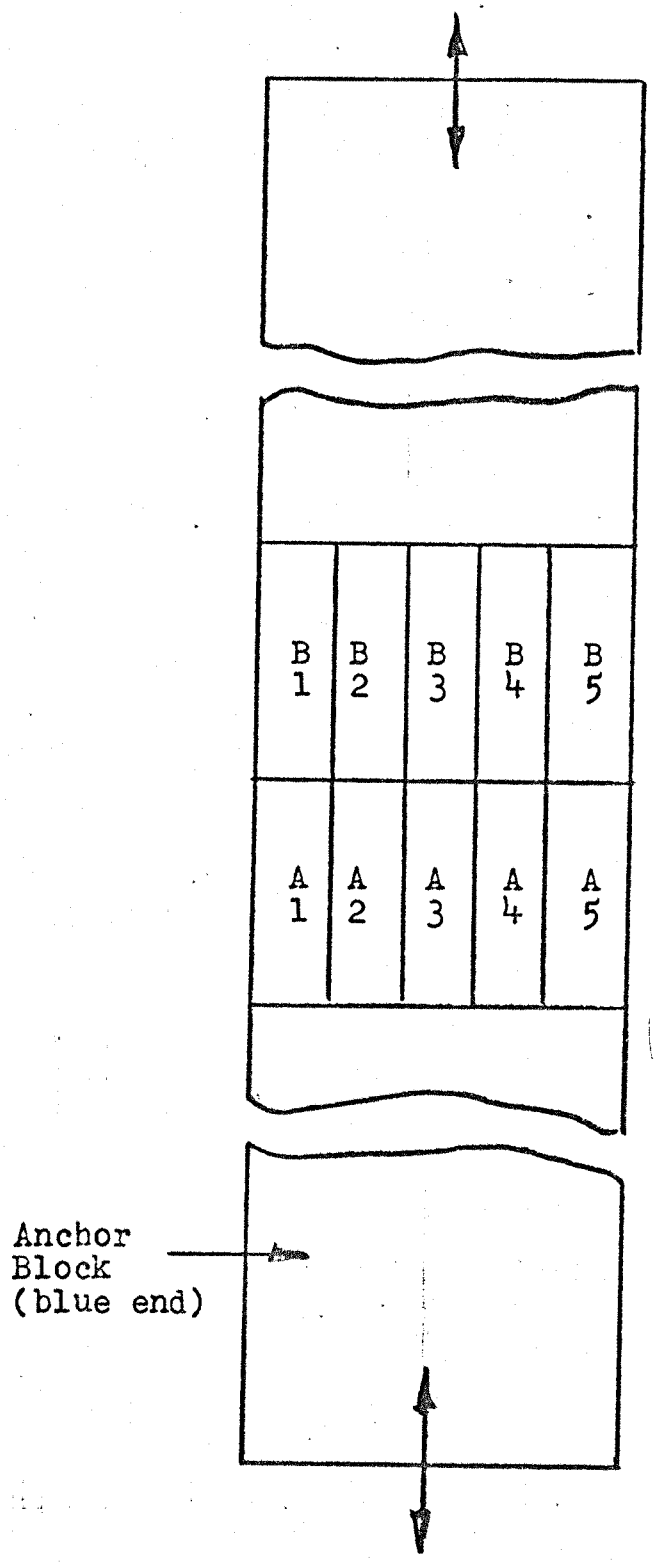

FIG. 18 POSITION OF NO PRESTRAIN (ZERO CYCLE) ROLLS - ROYCE - TYPE FATIGUE SPECIMENS.

CHAPTER 6

ROTATING CANTILEVER FATIGUE TEST RESULTS

6.1 Fatigue Test Pieces

Rotating bending fatigue tests were carried out using Rolls-Royce-Type specimens (Fig. 19) and S/N curves plotted for the unidirectional pre-strain ($\frac{1}{4}$ cycle). (Figs. 20 and 21). At a stress level of 232 MN/m^2 (15 ton/in^2) batches of each of samples from specimens 2,3 and 4 were fatigue tested. Fatigue results are given in Tables 2A, B, C and D and these have been analysed by a statistical method.

The stress level of 232 MN/m^2 (15 ton/in^2) was chosen for comparison as this appeared to be in a region in which changes in performance would be revealed without possible effects from discontinuities in the curve. (Figs. 20 and 21).

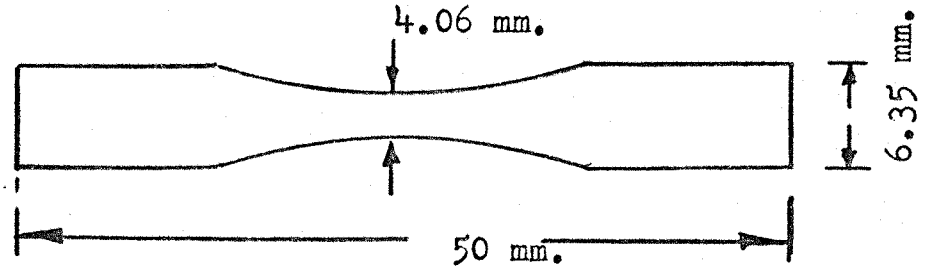

FIG. 19 ROLLS-ROYCE-TYPE FATIGUE SPECIMEN

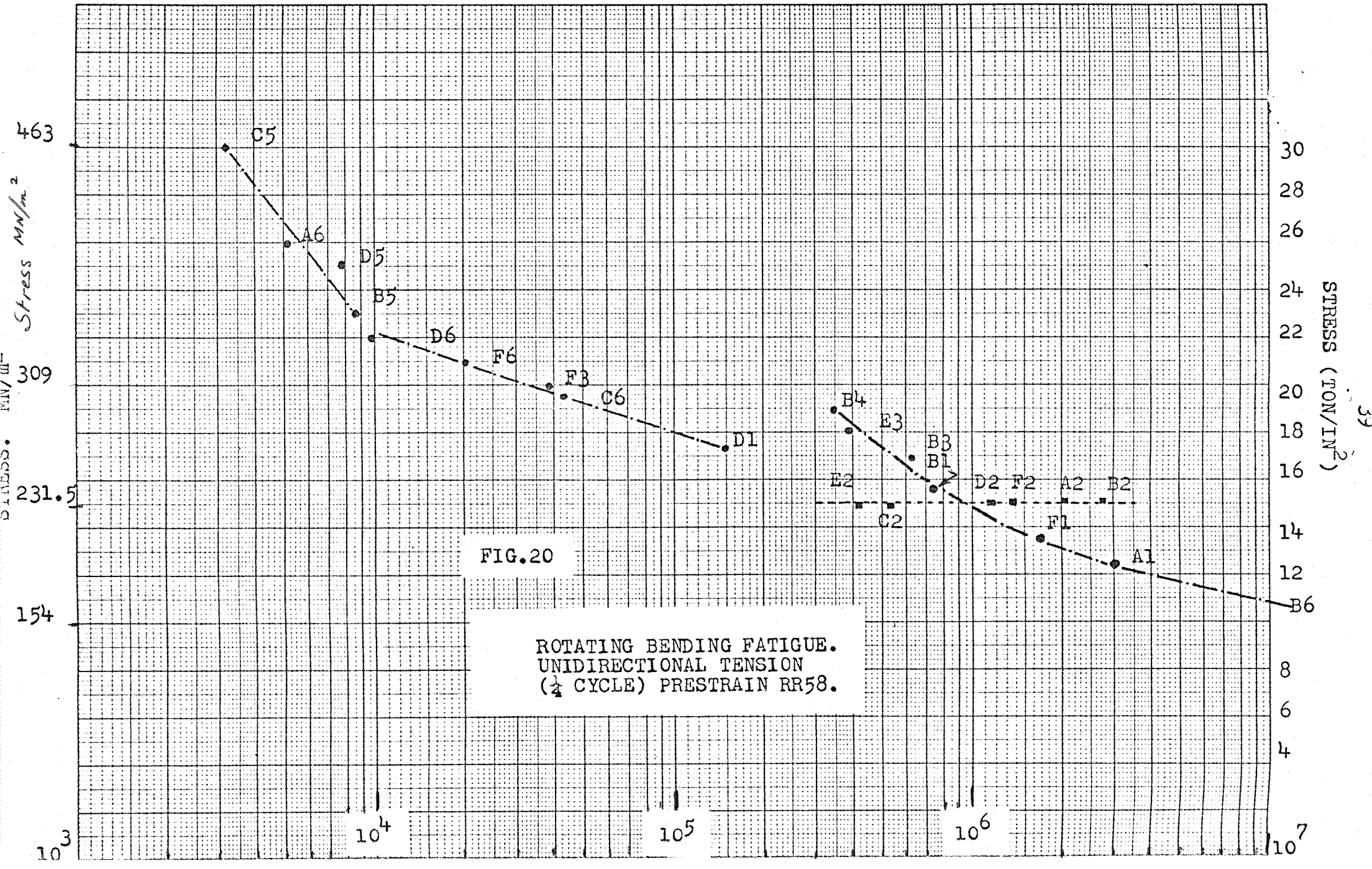

FIG.20

ROTATING BENDING FATIGUE.
UNIDIRECTIONAL TENSION
(¼ CYCLE) PRESTRAIN RR58.

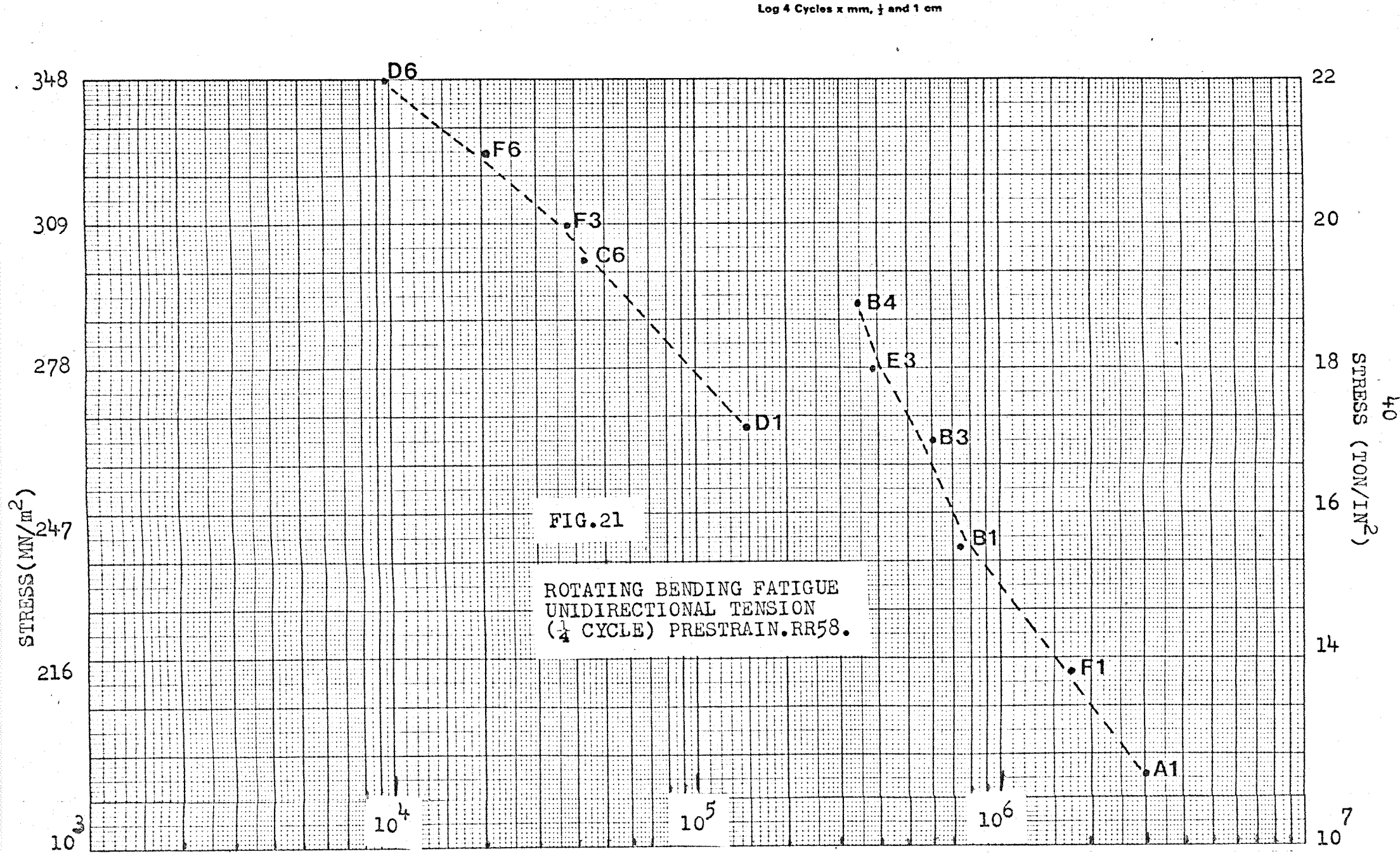
Log 4 Cycles x mm, ½ and 1 cm
348
309
278
247
216
10^3
10^4
10^5
10^6
10^7
STRESS (MN/m²)
STRESS (TON/IN²)
22
20
18
16
14
D6
F6
F3
C6
D1
B4
E3
B3
B1
F1
A1
FIG.21
ROTATING BENDING FATIGUE
UNIDIRECTIONAL TENSION
(¼ CYCLE) PRESTRAIN.RR58.

FATIGUE TEST RESULTS

6.2 TABLE 2A $\frac{1}{4}$ Cycle (Unidirectional Stretch Prior to Ageing)
Rotating Bending Fatigue

SPECIMEN NO.	STRESS MN/m^2	STRESS TON/in^2	CYCLES TO FAILURE ($\times 10^3$)
A1	190.68	12.35	3064
B1	239.32	15.5	749
C1	223.9	14.5	6893
D1			
E1			
F1	208.44	13.5	1733
A2	231.6	15	2054
B2	231.6	15	no test
C2	231.6	15	532.7
D2	231.6	15	1174.8
E2	231.6	15	417
F2	231.6	15	1330
A3	324.24	21	12.3
B3	262.5	17	63.9
E3	278	18	39.5
F3	309	20	39.3
A4	401.44	26	3.7
B4	293.36	19	34.7
F4	401.44	26	no test
A5	370.56	24	5.3
B5	355	23	8.6
C5	463	30	3.2
D5	386	25	7.8
E5	447.8	29	2.4
F5	416.9	27	2.4
A6	401.44	26	5.1
B6			
C6	301	19.5	442
D6	339.68	22	9.9
E6			
F6	324	21	208

FATIGUE TEST RESULTS

6.3 TABLE 2B 3 Cycle Pre-strain Prior to Ageing and Fatigue
Rotating Bending Fatigue

SPECIMEN NO.	STRESS MN/m^2	STRESS TON/in^2	CYCLES TO FAILURE ($\times 10^3$)
A1	231.6	15	237.6
A2	231.6	15	145.4
A4	231.6	15	270.5
A5	231.6	15	441
B1	231.6	15	251.7
B5	231.6	15	549

6.4 TABLE 2C 1000 Cycle Pre-strain Prior to Ageing and Fatigue
Rotating Bending Fatigue

SPECIMEN NO.	STRESS MN/m^2	STRESS TON/in^2	CYCLES TO FAILURE ($\times 10^3$)
C1	231.6	15	2610
C2	231.6	15	195.6
C3	231.6	15	263.3
C4	231.6	15	273.5
C5	231.6	15	412.5
D1	231.6	15	220.5
D5	231.6	15	357.1

FATIGUE TEST RESULTS

6.5 TABLE 2D No Pre-strain (Zero Cycle) Prior to Ageing and Fatigue Rotating Bending Fatigue

SPECIMEN NO.	STRESS MN/m^2	STRESS TON/in^2	CYCLES TO FAILURE ($\times 10^3$)
A1	231.6	15	411
A2	231.6	15	432.7
A3	231.6	15	463.4
A4	231.6	15	495.8
A5	231.6	15	503
B1	231.6	15	495

Statistical analysis of fatigue test results are given separately in this report.

CHAPTER 7

TENSILE TEST RESULTS

7.1 Solution Treated Condition

At the start of the work a tensile test was carried out on the RR58 test alloy in the solution treated condition to ascertain the 1% proof stress. (Fig. 22). This value of 262.5 MN/m^2 was used for the pre-strain of the test alloy prior to artificial ageing.

7.2 Pre-strained and Aged Condition

Tensile test specimens were made from some of the pre-strained and aged material of the large specimens 1, 2 and 3 (Item 5.2). These were restricted in size by the need to machine them from the same size rectangular blocks used for the Rolls Royce Type fatigue specimens.

Tensile test results for prestrained and aged material

TABLE 3

	Initial length	Final length	Diameter	Max. Load	U.T.S. MN/m^2	% Elong.
Unidirectional stretch ($\frac{1}{4}$ cycle)	50mm	54.75	4.32mm	4.7KN	320.8 (20.46)	9.5
3 cycle pre-strain	50mm	54	3.75	4.3	389 (24.8)	8.0
1000 cycle pre-strain	50mm	52.5	4.05	4.8	372.6 (23.8	5.0

It should be noted that the tests were not carried out on British Standard specimens and the percentage elongation was measured on overall length. Comparison should not therefore be made with percentage

FIG.22

TENSILE TEST
RR58 SOLUTION TREATED ONLY
Cross section 15.74 x 11.8 mm.
1% proof stress = 262.5 MN/m^2(17T/in^2)
Ultimate stress = 374 MN/m^2(24.2T/in^2)

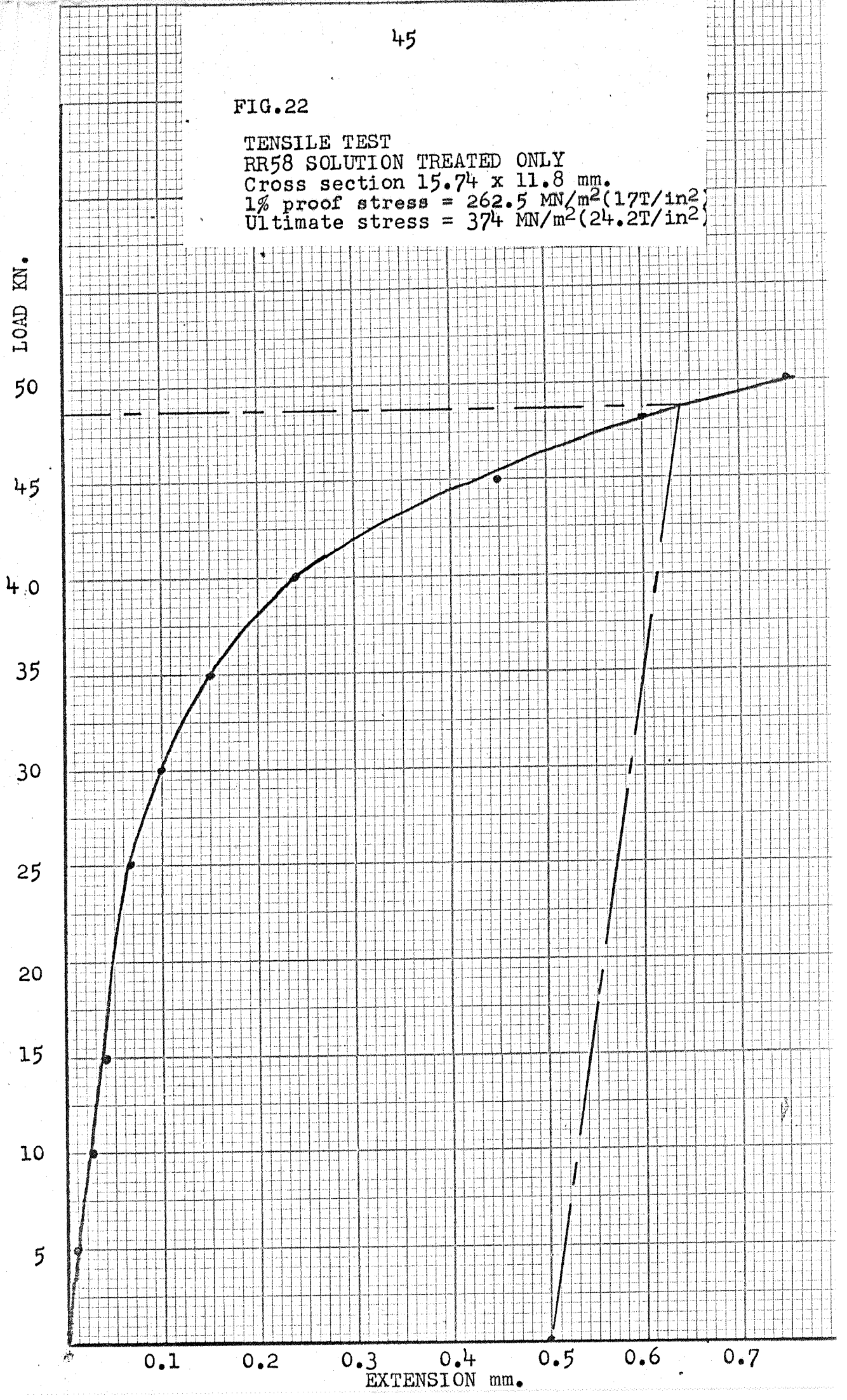

elongations on British Standard gauge lengths; the values obtained did however confirm loss of ductility with increased cold work. The increase in U.T.S. of the cyclically pre-strained specimens compared with the less cold worked $\frac{1}{4}$ cycle was also confirmed. No significance was attached to the lowering of U.T.S. from 389 MN/m^2 (24.8 ton/in^2) to 372.6 MN/m^2 (23.8 ton/in^2) for the 3 cycle to the 1000 cycle pre-strain respectively as imperfections in machining these small specimens may account for the fall.

CHAPTER 8

ELECTRICAL CONDUCTIVITY MEASUREMENTS

Age hardening of the test alloy was carried out for 19½ hours at 190°C. In order to examine the sensitivity of the material to the age hardening time the unidirectional stretch (¼ cycle pre-strain) sample was aged at various times. The 3 cycle and 1000 cycle samples could not be examined as all of the sample had been used in fatigue tests and tensile tests. For the ¼ cycle pre-strained material the variation in hardness and conductivity was measured.

Hardness measurements were made using VHN and Rockwell.

The % IACS conductivity was measured using an Electrical Conduction Novamho Type 101 machine made by Novalec Ltd. Twickenham, England.

TABLE 4 Artificial Ageing Time - % IACS (¼ cycle pre-strain)

Hours at 190°C	% IACS conductivity	VHN
13	38½	129
15	40¼	129
16	39½	129
17	40⅝	130
18	41½	130
19	41½	131
20	42½	130
23	42	131
42½	42½	129

The values appeared to be on a plateau over the time tested. If the peak hardness had been brought forward in ageing time by pre-strain then it is possible that all values were obtained for material at about

peak hardness. Further investigation is warranted since it is well known that cold working alters ageing characteristics and this was a somewhat surprising result. As referred to in the discussion Gayler found for an aluminium alloy subjected to cold work a reduction of ageing time to peak value from 8 hours to 55 minutes.

CHAPTER 9

MICROSCOPICAL EXAMINATION

9.1 General

The artificially aged specimens of unidirectional stretch, 3 cycle, 1000 cycle and Zero cycle (no pre-strain) RR58 were mounted both cold and in bakelite and polished using a Disa Electropol machine. Etching was carried out by Kellers Etch, 2% HF + 10% 50/50 HCL/water.

These were examined in a Vickers Microscope.

The small size of the Rolls-Royce-Type fatigue specimens necessitated mounting. Heat associated with the mounting as used with bakelite was not considered satisfactory as it introduced another factor. With cold mounting using the rotating bending fatigue specimens there was difficulty in associating the fracture with the macro structure. It was therefore decided to examine the fractures using an electron scanning microscope (Stereoscan), and to examine the effects of any pre-strain on ageing and the structure using an Electron Microscope and thin foils.

9.2 Preparation of Specimens for Electron Microscopy

Thin foil microscopy was used throughout.

The ends of the fatigue specimens in rotating bending were used to examine the unfatigued as well as the fatigued regions. Due to the round shape of the fractured fatigue specimens and the need to machine to a flat disc, the irregular fracture surface could not be examined by this technique and the Stereoscan electron scanning microscope was used for examining of the actual fracture surface.

Thin foils could however be prepared for the area adjoining the

fracture in the rotating bending specimens. The circular cross section at the fatigue fracture was first machined flat and then reduced to 3 mm diameter.

Thin microfoil slices were then cut off this cylinder using a MICROSLICE made by Metals Research Ltd. Cambridge, England. Longitudinal strips running into the fracture surface were also prepared and after thinning by abrasion 3 mm diameter discs were punched from these.

Final thinning of all discs was carried out using a STRUERS TENEPOL machine made in Denmark (Agent : Vickers,Coulsdon, Surrey) until perforations appeared.

The electrolyte used consisted of 20% nitric acid by volume in ethyl alcohol. The microfoils were washed in acetone. The foils were kept in a dessicator until examined in the electron microscope. Micrographs were taken and are referred to in the discussion. The electron microscope used was a JEOL (JEM 200A) EM-BGMZ. The use of the electron microscope is well described in current literature.

9.3 Electron Micrographs of Fine Microstructure

Thin foil electron microscopy confirmed the formation of a substructure and indicated the grain boundaries in detail as shown in Plates 7 to 10. Plate 11 shows a precipitate depleted zone. The interpretation of these features and their importance to the subsequent fatigue behaviour are discussed later.

9.4 Electron Scanning Microscope (STEREOSCAN) Fractographs

Typical features revealed by the electron micrographs are shown by Plates 1-6, 12-15. These include striations and secondary cracks, the interpretation of which are discussed later.

9.5 Optical Microscopical Examination of Fatigue Features

It was considered that on a macro scale the examination of the fatigue fractures in relation to the structure of the alloy could be carried out more favourably using strip specimens in reverse bending fatigue. Flat strips of the unidirectional ($\frac{1}{4}$ cycle), 3 cycle and 1000 cycle pre-strained and aged material were therefore polished, fatigue tested and examined in the Vickers Microscope and photographed. The ends of the fractures were also examined using the electron scanning microscope. The flat strips were polished using a Disa Electropol machine and the additional programme of fatigue testing (in reverse bending) was carried out using a Carl Schenck/Avery type machine.

Plate 16 shows the irregularity of the fracture surface. Optical examination of the aged material in the Vickers Microscope showed that precipitated slip bands as normally observed in stretched plate had developed in the material with unidirectional stretch i.e. $\frac{1}{4}$ cycle but the material pre-strained with 1000 cycles had developed a substructure as shown in Plates 17 and 18.

CHAPTER 10

STATISTICAL EXAMINATION OF FATIGUE RESULTS

There are various recommendations for the statistical examination of test results (B.S.3518; B.S.600., Revue de Soudure 1958, Vol. 14, p. 24-32).

10.1 Types of Error

In fatigue testing since generally a relative small number of test pieces are used to represent a much larger group, precautions must be taken to control the effect of error on the test material and on comparisons to be made.

Errors are likely to arise to some extent at stages of sampling, test piece preparation and testing. Statistical techniques are used to (1) estimate the parameters once having assumed that log life has normal distribution. (2) examine the causes predicted by the engineer. Two types of errors which occur at stages of selection, heat treatment, processing and the preparation and testing of test pieces are systematic errors and random errors.

Systematic errors are those which persist irrespective of the number of samples e.g. when material A is given treatment 1 and material B receives treatment 2 it is not possible to establish whether differences in the two sets of results are due to differences in the materials or due to differences in the treatments.

Random errors are those arising by chance events over which the experimenter has no control. For these statistical methods are most appropriate.

It is necessary for the experimenter to evaluate the relative importance of the various sources of variation. Randomisation and replication are used to control the effects of error. Randomisation is used to safeguard against unsuspected patterns of variation e.g. along a bar of material. For this reason a record was kept of the pattern of fatigue specimens cut from the bulk sample. Randomisation may be used to allocate the order of preparation and treatments given to samples. This was considered unnecessary in the preparation of test specimens as use was made of refrigeration to restrict variation.

The need to pre-strain the bulk samples restricted the size of the bulk sample to the capacity of the Losenhausen Machine (600 KN). The number of fatigue specimens and tensile specimens that could be machined from each of the different pre-strain samples was therefore restricted but as far as possible replication was used. Replication permits the estimate of random error from the comparison of different test pieces exposed independently to the same conditions so reducing the effect of random variability. For this reason sets of fatigue specimens in rotating bending were used for each of the unidirectional stretch ($\frac{1}{4}$ cycle), 3 cycle, 1000 cycle and no pre-strain samples at a comparison level of 231.6 MN/m^2 stress (15 ton/in^2).

Accuracy

Whatever statistical technique is applied it cannot give results any more accurate than the original accuracy of the test data. The accuracy required should thus be decided when planning the tests. In the tensile tests on the pre-strained and aged material larger test specimens to B. Standards were preferable but limitations on the size of the bulk samples used for cutting into fatigue specimens, due to the

capacity of the Losenhausen machine for pre-strain cycling (600 KN-60 ton), restricted the size of the test specimens.

Distribution Curves

Many facts and test results can be fitted to a curve called a distribution curve. There are a number of such curves such as:-

10.2 (1) The Normal Frequency Distribution
(or Gaussian Frequency Distribution)

Natural phenomena often suit this distribution which is widely used.

An appropriate statistical distribution for fatigue data is one with a tail extending over a great range of cycles forming a displacement from the normal (Gaussian) distribution. This is called a skew distribution and a number of theoretical distributions give this shape.

A commonly used method for the analysis of skew distributions when all test pieces fracture is to use the logarithm of the cycles to failure and use 'log-life' as if distributed normally. This is an empirical technique.

A commonly used method for determining whether a frequency distribution is acceptable as a normal distribution is to plot results of cumulative frequency distribution on normal probability paper and to check that it gives an approximate straight line.[76] The goodness of fit of the test results to the normal distribution is measured using the 'Chi-Square' test.

10.3 (2) Students 't' Distribution

When a small number of samples (n less than 25) is used then Students 't' distribution analogous to the normal distribution but

allowing for a greater element of uncertainty due to the small number of test results is often used. Values of the 't' distribution corresponding to different degrees of freedom and significance levels were first worked out by (Student) W.S. Gosset and proved by R.A. Fisher.

For small samples it is found that an unbiased estimate of the variance and hence the standard deviation is found by using (n - 1) as the denominator in the variance instead of 'n' (size of sample) as is done with the normal distribution. The symbol 'S' is often used for the standard deviation when (n - 1) is being used.

The degrees of freedom = (n - 1) where n is the size of sample. 't' distribution values for various levels of significance (e.g. 5%) are available in various publications. (Biometrika Tables; Statistical Methods for Research Workers by R.A. Fisher published by Oliver & Boyd Ltd. Edinburgh). The 't' distribution was used in the analysis of test data in this report.

10.4 (3) Weibull Distribution

The distribution for which there is most theoretical justification is called the Weibull distribution which resembles the cumulative distribution curve of the normal distribution but has a finite lower limit.

It is sometimes used to describe the yield strength distribution of steel and fatigue life at constant stress. It is quoted as being particularly well suited to describing the distribution of the fatigue life of bearings[76,77].

It was not considered appropriate in the present tests due to the small size of the sample and Students 't' distribution which corrects for the small size of sample, as explained earlier, was used.

(4) Other Distributions

There are a number of other distributions including the Poisson, the Binomial, the Rectangular and the Cauchy. The Poisson and the Normal Distribution referred to above are special cases of the Binomial Distribution which has the fundamental distribution from the theoretical point of view.

10.5 Terms Used in Statistical Analysis

X^2 (Chi-squared) test - a statistical test used to discover whether the observed frequencies of events differ significantly from their expected values. The significance of the relation between two members of the sample is established by setting out a contingency table and applying the chi-squared distribution and the 5% (or other) significance level.

Degrees of Freedom - if there are 'n' observations the quantity $(n - 1)$ is used for the degrees of freedom. It is equal to the number of observations minus the number of linear relations between the observations. Since although the test results are independent they are linked by the arithmetic mean which is one linear relation between them and hence one is taken from the number of observations to give $(n - 1)$.

Measures of position on a curve are the mean (arithmetic mean) and the median.

The MEAN (ARITHMETIC MEAN) of a set of readings N_1 N_2 ... N_n

$$\text{is } \bar{N} = \frac{N_1 + N_2 \cdots N_n}{n}$$

where n = number of readings or test pieces.

The MEDIAN is the middle value of the readings N_1 N_2 etc. if n is ODD but is the average of the two middle readings if n is EVEN.

MEASURES OF SCATTER are the variance, the standard deviation and the range.

STANDARD DEVIATION is a measure of the dispersion of a frequency distribution (the square root of the variance).

The VARIANCE is the mean of the deviations from the mean (mean = $\frac{\Sigma N}{n}$ The variance of a group of 'n' measures N_1 N_2 ... etc. is

$$\sigma^2 = \frac{(N_1 - \bar{N})^2 + (N_2 - \bar{N})^2 \ldots\ldots}{n}$$

where $\bar{N}$ = arithmetic mean $\frac{\Sigma N}{n}$

when $n < 30$ this is written

$$S^2 = \frac{(N_1 - \bar{N})^2 + (N_2 - \bar{N})^2 \ldots\ldots}{(n - 1)}$$

σ being renamed S to indicate that $(n - 1)$ is used as the denominator.

This modification to the formula allows for greater possible errors due to the use of a small sample.

$$\text{Thus } S^2 = \frac{\Sigma(N - \bar{N})^2}{n - 1} = \text{VARIANCE}$$

$$S = \text{STANDARD DEVIATION} = \sqrt{\text{VARIANCE}}$$

S^2 can also be calculated from the formula

$S^2 = \frac{\Sigma N^2}{n - 1} - \bar{N}^2$ which can be shown to be the same as the above.

RANGE. If the range is (a - b) then N = a and N = b are the smallest and largest values of the variate in the measurement.

10.6 Analyses of Fatigue Results of Tables 2A, B, C, D.

The stress level used for comparison was 231.6 MN/m^2 (15 ton/in^2) and there were six readings for each of no pre-strain (Zero cycle), unidirectional stretch ($\frac{1}{4}$ cycle), 3 cycle and 1000 cycle pre-strain for the analyses.

The Log-normal distribution was used based on Revue de Soudure 1958 Vol. 14, p. 24-32 the formulae being

$$\text{ARITHMETIC MEAN (Mean value) LOG } \bar{N} = \frac{\Sigma \text{LOG } N}{n}$$

$$\text{VARIANCE } S^2 = \frac{\Sigma (\text{LOG } N - \text{LOG } \bar{N})^2}{n - 1}$$

$$\text{STANDARD DEVIATION } \sigma = \frac{S}{b_n} \sqrt{\frac{n - 1}{n}}$$

The square root quantity in the standard deviation is equivalent to the using of n instead of n - 1 in the variance as frequently used where the sample is small. The normal answer is corrected for the very small sample by dividing by the value b_n which appears in the publication referred to earlier, used in conjunction with STUDENTS 't' values.

N = number of cycles to rupture

n = number of test pieces

σ = standard deviation

Effect of plastic deformation prior to ageing on the fatigue strength of aluminium alloy RR58

Table 5 $\frac{1}{4}$ (unidirectional tensile) and 3 cycles pre-strain

	Endurance N $\frac{1}{4}$ cycle ($\times 10^5$)	Log N $\frac{1}{4}$ cycle	Endurance N 3 cycles ($\times 10^5$)	Log N 3 cycles
	13.33	6.12385	2.7	5.43136
	11.7	6.06819	1.45	5.16137
	5.32	5.72591	2.52	5.40140
	4.17	5.62041	4.4	5.64345
	20.5	6.31175	2.37	5.37475
	27.8	6.44404	5.49	5.73957
Σ N	82.79		18.93	
Σ Log N		36.2936		32.7516
Σ N/n	13.798		3.155	
Σ (Log N/n)		6.0489		5.4586
σ	0.3386		0.2163	

When n = 6 $\quad \sigma = \frac{S}{b_n}\sqrt{\frac{5}{6}} = 0.913\,\frac{S}{b_n}$

where $b_n = 0.869$ for 6 specimens

Table 6 1000 cycles and no pre-strain

	Endurance N 1000 cycles ($\times 10^5$)	Log N 1000 cycle	Endurance N No pre-strain ($\times 10^5$)	Log N No pre-strain
	2.74	5.43775	4.11	5.61384
	2.63	5.41996	4.327	5.63649
	1.96	5.29226	4.634	5.6656
	3.57	5.55267	5.958	5.77525
	2.2	5.34242	5.03	5.7016
	4.1	5.61278	4.95	5.6946
Σ N	17.2		29.0	
Σ Log N		32.6575		34.0874
Σ N/n	2.867		4.8348	
Σ (Log N/n)		5.4429		5.68
σ	0.128		0.0613	

where $\sigma = \frac{0.913\ S}{b_n}$ with b_n = 0.869 for 6 specimens as previous table

Table 7 Summary

	$\frac{1}{4}$ cycle	3 cycles	1000 cycles	No pre-strain
Average endurance Σ N/n ($\times 10^6$)	1.3798	0.3155	0.2867	0.484
Standard Deviation	0.3386	0.2163	0.1280	0.0613

PROBABILITIES

B.S.3418 page 14 Probability of failure given by $\frac{\text{index i}}{n + 1}$

Table 8A $\frac{1}{4}$ Cycle (Unidirectional Stretch)

INDEX i	Number of cycles to rupture N ($\times 10^5$)	LOG N	$\frac{i}{n+1}$
1	4.17	5.62041	0.142
2	5.32	5.72591	0.284
3	11.7	6.06819	0.426
4	13.3	6.12385	0.568
5	20.5	6.31175	0.710
6	27.8	6.44404	0.852

Table 8B 3 Cycle Pre-strain

INDEX i	Number of cycles to rupture N ($\times 10^5$)	LOG N	$\frac{i}{n+1}$
1	1.45	5.16137	0.142
2	2.37	5.37475	0.284
3	2.52	5.40140	0.426
4	2.7	5.43136	0.568
5	4.4	5.64345	0.710
6	5.49	5.73957	0.852

Table 8C 1000 Cycle Pre-strain

INDEX i	Number of cycles to rupture N ($\times 10^5$)	LOG N	$\frac{i}{n+1}$
1	1.96	5.29226	0.142
2	2.2	5.34242	0.284
3	2.63	5.41996	0.426
4	2.74	5.43775	0.568
5	3.57	5.55267	0.710
6	4.1	5.61278	0.852

Table 8D No Pre-strain

INDEX i	Number of cycles to rupture N ($\times 10^5$)	LOG N	$\frac{i}{n+1}$
1	4.11	5.61384	0.142
2	4.327	5.63649	0.284
3	4.634	5.6656	0.426
4	4.95	5.6946	0.568
5	5.03	5.7016	0.710
6	5.958	5.77525	0.852

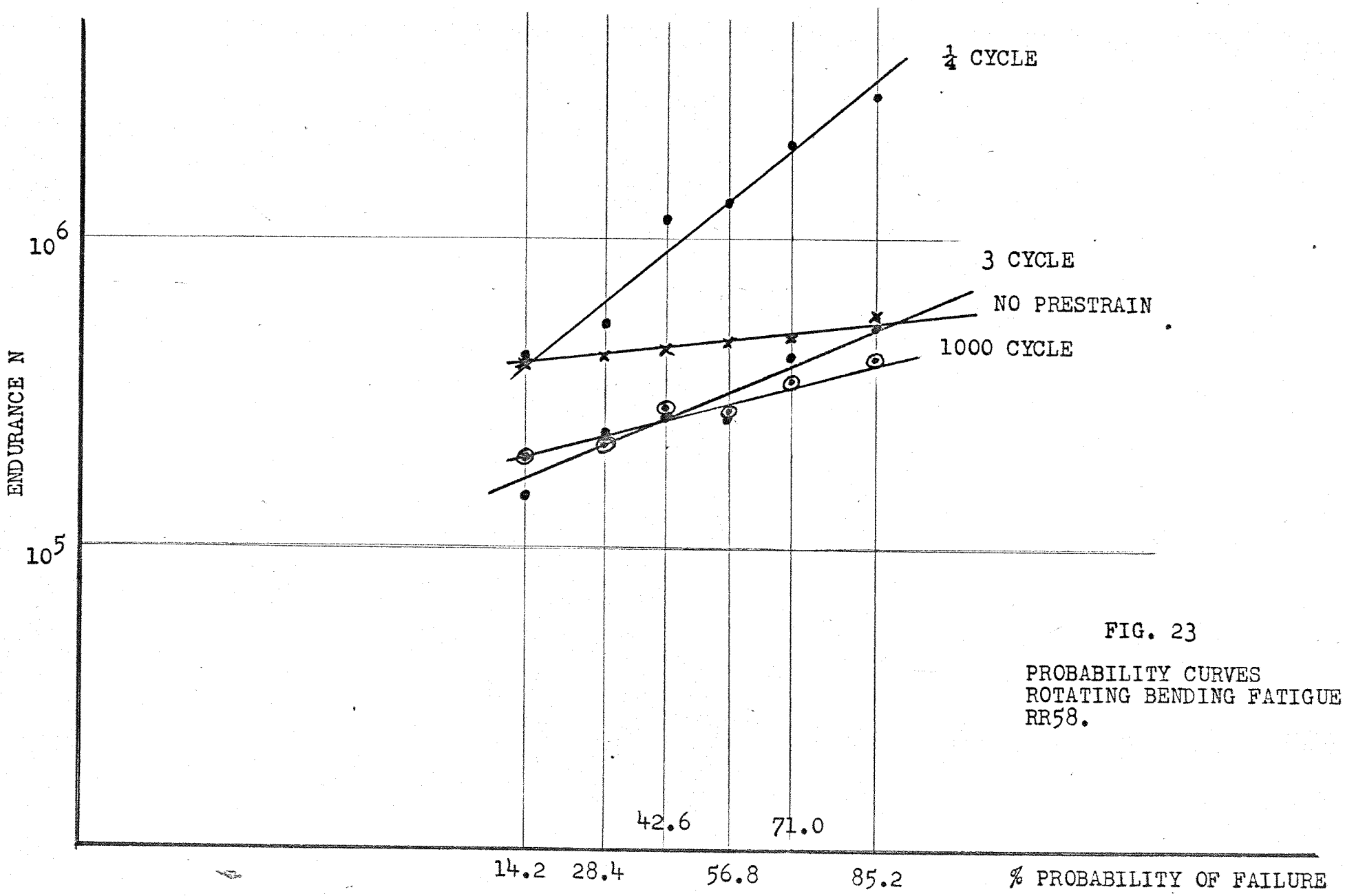

FIG. 23

PROBABILITY CURVES
ROTATING BENDING FATIGUE
RR58.

CHAPTER 11

DISCUSSION

The statistical analysis showed that for a given stress the fatigue life increased with unidirectional pre-strain but was reduced by cyclic pre-strain, and in this respect 3 cycles were almost as damaging as 1000 cycles. Whilst these effects were significant but not sufficiently great to be of immediate interest it was hoped that some explanation might be forthcoming from differences in macrostructure and microstructure in relation to fatigue mechanisms.

An optical microscopical examination of aged material with the three conditions of pre-strain showed that the unidirectional i.e. $\frac{1}{4}$ cycle pre-strained material had developed precipitated slip bands as normally observed in pre-stretched plate, but the material that had received 1000 cycles pre-strain had developed a substructure as shown in Plates 17 and 18. Thin foil electron microscopy confirmed the presence of this substructure and showed the nature of the subgrain boundaries in some detail. Examples are shown in Plates 7 to 10 where it can be seen that precipitation has occurred, although presumably because of the small disorientations, this is less clearly defined than the coarse main grain boundary precipitates such as are illustrated in Plate 11.

Fatigue deformation is known to produce unique dislocation defect structures not observed with unidirectional strain. One characteristic of fatigue at relatively low strain levels is the localisation of the heaviest deformation into well defined bands, but at higher strains, particularly in high stacking fault energy materials, the deformation becomes more uniformly spread and a substructure may be formed with

boundary walls containing dislocation loops etc. surrounding practically dislocation free subgrains.

In order to produce the most homogeneous deformation a high fatigue pre-strain level was chosen although the principle was that the fatigue strains would in any case act preferably at metallurgical stress concentrations and thereby provide maximum benefit by inducing more effective precipitation hardening in these places that might otherwise be weak in fatigue.

The idea behind the work of Stubbington[17] was to induce more effective precipitate nucleation which was particularly advantageous with his Al-Mg alloy. It is clear that if a substructure is produced by the high fatigue strain, although the general deformation has been homogenised, it has produced a cellular structure involving the defects which are effectively partitioned from the defect free cells. This structural network may have properties, independent of the matrix, and differing from a more loosely tangled dislocation structure such as produced by the unidirectional strain. There is evidence that this is so e.g. creep.

Nevertheless the precipitated structure does increase the tensile strength but fatigue, always picking on the weak points, would be more sensitive to any inhomogeneity. It appears that the evidence of the present work reveals that sub-boundaries and main grain boundaries are weak paths along which fatigue crack can develop easily as shown in Plate 19.

The regions in the vicinity of grain and sub-grain boundaries often become a precipitate free zone or a precipitate depleted zone and there is some evidence of this in the micrographs (Plate 11). The boundaries consisting of a brittle precipitate may themselves form a favourable path for a crack. The precipitate depleted zone, being softer, may

encourage local plastic strain that would increase the boundary stress at local points.

The sub-grain boundary path accounts for the irregularity of the fracture surface shown in Plate 19 (optical fractograph) and Plates 12 and 20. Ductile growth striations were evident where the crack growth rate was high as shown in Plate 15, but at lower rates the fracture appeared typically as shown in Plates 12 and 13, the latter also showing secondary crack evidence as described by Gauthier et al[78] (Engineering Fracture Mechanics 1973, Vol. 5, p. 977-981).

Patterns of lines called striations are often exhibited by fatigue fractures as shown by the electron micrographs (Plates 1 to 6). These striations represent the successive positions of the crack front during propagation. One striation is formed per cycle and its presence indicates that the material at the crack tip has deformed plastically. It is necessary to distinguish true fatigue striations from other features which have a somewhat similar appearance e.g. slip bands and so called 'tyre marks'.

Little can be said about the effect of the pre-strain on the rate of age hardening because the 'plateau' hardness appeared to be quickly reached in less than 13 hours and this was confirmed by the almost constant conductivity measurements. This was somewhat surprising and no explanation was found for this behaviour.

Having stated that the production of substructure appears to be a detrimental feature as regards subsequent fatigue strength it is of interest to speculate on what the properties would have been (a) if the pre-strain fatigue had been less or (b) a shorter ageing time had been used.

CONCLUSIONS

1. Unidirectional tensile stress of value equal to the 1% proof stress, applied between solution treatment and artificial ageing slightly improved the fatigue strength of the RR58 aluminium alloy, and therefore the practice of straightening the alloy during manufacture, in the solution treated condition, would not appear to be harmful to fatigue life provided that this is achieved by tensile stress.

2. Cyclic pre-strain (R = -1) of the same stress value, introduced between solution treatment and artificial ageing produced a significant loss in fatigue resistance of the material, and in this respect 3 cycles were almost as damaging as 1000 cycles pre-strain.

3. Pre-strain introduced between solution treatment and ageing influences the subsequent precipitation in such a manner that the ageing times and temperatures to produce optimum fatigue life may need adjustment.

4. Cyclic pre-strain and subsequent artificial ageing produced sub-grain boundaries containing precipitates and with associated precipitate depleted zones.

5. The grain and sub-grain boundaries with their adjoining precipitate depleted zones offered lower resistance to fatigue crack growth than the matrix.

6. The cyclically pre-strained material which exhibited substructure had a higher U.T.S. than the unidirectionally stretched material, which is a reversal from the fatigue strength.

SUGGESTIONS FOR FURTHER WORK

Further work is necessary to determine the effects of varying the pre-strain and the subsequent ageing conditions. There may well be an optimum combination that would improve fatigue properties. Perhaps some thought could be given to alloying conditions.

REFERENCES

1. J.M. Silcock - J. Inst. Metals 1961, 89 203
2. R.N. Wilson and P.J.E. Forsyth - J. Inst. Metals 1966, 94 8
3. I.J. Polmear - Trans. Met. Sc. A.I.M.E. 1964, 230 1331
4. G. Thomas - Phil. Mag. 1959, 4 1213
5. G. Thomas and M.J. Whelan - Phil. Mag. 1959, 4 511
6. Yu. A. Bagaryatsky - Fulmer Research Inst. Translations Nos. 11, 12, 55 and 66
7. V. Gerold and H. Haberkorn - Z. Metallkunde 1959, 50 568
8. G. Thomas - Phil. Mag. 1961-2, 90 57
9. D. Pashley, J. Rhodes and A. Sondorek - J. Inst. Metals 1966, 94 41
10. F.R.N. Nabarro - Proc. Roy. Soc. 52 1940, 90
11. R.N. Wilson, D.M. Moore and P.J.E. Forsyth - J. Inst. Metals 1967, 95 177
12. R.N. Wilson and P.G. Partridge - Acta Metall. Vol. 13, 1965, 1321
13. D. Vaughan - Ref. 4 of 2
14. G.B. Brook and B.A. Parsons - Fulmer Research Inst. Rep. R207/1 1964
15. N. Sen and D.R.F. West - Ph.D. Thesis Univ. London, 1967
16. G.C. Weatherly and R.B. Nicholson - Min. Aviation D. Mat. Progress Rep. PD/25/025 1964
17. C.A. Stubbington - J. Inst. Metals 1959-60, Vol. 88, p. 227
18. A. Kelly and R.B. Nicholson - Progress in Materials Science, Vol. 10 p. 243
19. A. Perlitz and A. Westgren - Arkiv. Kemi. Min. Geol. B. 1943, 16 13
20. J. Moulins and D. Adenis - Rev. de L'aluminium Sept. 1967, 937
21. M.A. Dewey - Acon Lab. Rep. 318/10 1963
22. H. Hardy - J. Inst. Metals 1954, 83 17
23. R.W. Lindsay and J. Norton - Trans. A.I.M.M.E. 1939, 133 111
24. M.L. Gayler - J. Inst. Metals 1946, 72 543

25. G. Thomas and J. Washburn - Rev. Modern Physics 1963, 35 992

26. A. Kelly and R.B. Nicholson - Ref. 18, p. 151

27. R.M.J. Cotterill, M. Doyama, J. Jackson and M. Sheshii - Lattice Defects in Quenched Materials Academic Press, 1965

28. J. Moulins, D. Adenis and R. Develay - Influence de l'attente entre trempe et revenue sur la precipitation. Memoires Scientifiques Rev. Met. LXVI No. 12, 1969

29. T. Broom and A. Nicholson - Adv. Physics 1954, 3 26, J. Inst. Metals 1960-1, 89 183

30. J.A. Ewing and J.C.W. Humfrey - Phil. Trans. A. Vol. 200 1903, 241

31. W.J. Plumbridge and D.A. Ryder - Met. Rev. 136 1969

32. N. Thompson and N.J. Wadsworth - Advances in Physics 1958, 7, 72

33. D. Walton and E.G. Ellison - Fatigue crack initiation and propagation Int. Met. Rev. 163 (1972)

34. R.K. Ham - Thermal and high strain fatigue p. 55, 1967 : London Inst. Metals.

35. C. Laird - "Fatigue crack propagation", A.S.T.M. STP 415, (1967) p. 139

36. J.R. Low - "Fracture of Solids" p. 167, (1963), Interscience Publishers

37. D.H. Avery and W.A. Backofen - ibid., p. 339

38. J.C. Grosskreutz - 'Fatigue - An Interdisciplinary Approach' p. 27, 1964 Syracuse, N.Y. University Press

39. S.S. Manson - J. Exper. Mechanics, 1965, 5 193

40. Proceedings of the International Conference on Mechanisms of Fatigue in Crystalline Solids, Orlando, Florida, 1962. Acta Met., 1963, 11, 643

41. Proceedings of the Crack Propagation Symposium, Cranfield 1961. College of Aeronautics

42. Proc. 1st Internat. Conf. Fracture (Sendai, Japan), 1965

43. 'Fracture' (Proceedings of the 1st Tewkesbury Symposium), 1965, London (Butterworths)

44. P.J.E. Forsyth and D.A. Ryder - Metallurgia 1961, 63, 117

45. P. Forsyth - Ref. 41, pp. 76, 484 and Acta Met. 1963, 11, 703

46. P.J.E. Forsyth - Nature, 1953, 171, 172

47. P.J.E. Forsyth - J. Inst. Metals 1954-55, 83, 395

48. A.H. Cottrell and D. Hull - Proc. Roy. Soc., 1957 (A) 242, 211

49. P.J.E. Forsyth - Proc. Roy. Soc. 1957 (A) Vol. 242, p. 198

50. P.J.E. Forsyth - ibid., p. 200

51. P.J.E. Forsyth - Acta. Met. Vol. 2, No. 7, July 1963, 203

53. Golland and James - Met. Science J. 4, p. 113, 1970

54. P.J.E. Forsyth, C.A. Stubbington and R.N. Wilson - R.A.E. Estab. Tech. Note (Met/Phys. 333) 1961

55. P.J.E. Forsyth and C.A. Stubbington (Met/Phys. 344)

56. C. Laird - "Fatigue Crack Propagation" - A.S.T.M., STP 415, 1967, p. 131

57. P.J.E. Forsyth and D.A. Ryder - Metallurgia, 1961, 63 117

58. R.W. Hertzberg - "Fatigue Crack Propagation". A.S.T.M., STP 415, 1967, p. 205

59. A.J. McEvily and R.C. Boettner - J.R. Low "Fracture of Solids" 1963, p. 383, and Acta. Met. Vol. 11, July 1963, and p. 383 of Ref. 62

60. D.S. Kemsley - J. Inst. Metals 1956-7, 85, 820

61. G.C. Smith - Proc. Roy. Soc. 1957 (A) 242, 189

62. A.J. McEvily and R.C. Boettner. J.R. Low "Fracture of Solids" 1963, p. 197

63. C.A. Stubbington and P.J.E. Forsyth - J. Inst. Metals 1957-8, 86, 90

64. H.J. Gough - Proc. Amer. Soc. Test. Mat. 1933, 33, 33

65. P.G. Partridge - Acta. Met. 1965, 13, 517

66. W.A. Wood - 'Fracture' p. 376, 1959

67. M.J. May and R.W.K. Honeycombe - J. Inst. Metals 1963-4, 92, 41

68. J.B. Clark and A.J. McEvily - Acta. Met., 1964, 12, 1359

69. C.A. Stubbington - Acta. Met. 1964, 12, 931

70. C.A. Stubbington and P.J.E. Forsyth - Acta. Met. 1966, 14, 5

71. R.N. Wilson and P.J.E. Forsyth - J. Inst. Metals. 87, 336, 1959

72. J.C. Grosskreutz and P. Waldow - Acta. Met. Vol. 11, 1963

73. Ref. 72, pages 3, 9-11, 17, 35

74. G.Y. Chin and W.A. Backofen - J. Inst. Metals, 90, 11 (1961)

75. J.C. Grosskreutz - J. App. Physics 33, 1787, (1962)

76. 'Mechanical Metallurgy' Dieter, McGraw Hill

77. Lieblein and Zelen - J. Research Natl. Bur. Stdrs. Vol. 57, p. 273-316, 1956

78. Engineering Fracture Mechanics Vol. 5, p. 977-981, (1973)

PLATE 1 1000 CYCLE PRESTRAIN BETWEEN S.T. AND AGEING.FATIGUED.(STEREOSCAN x 2.2K)

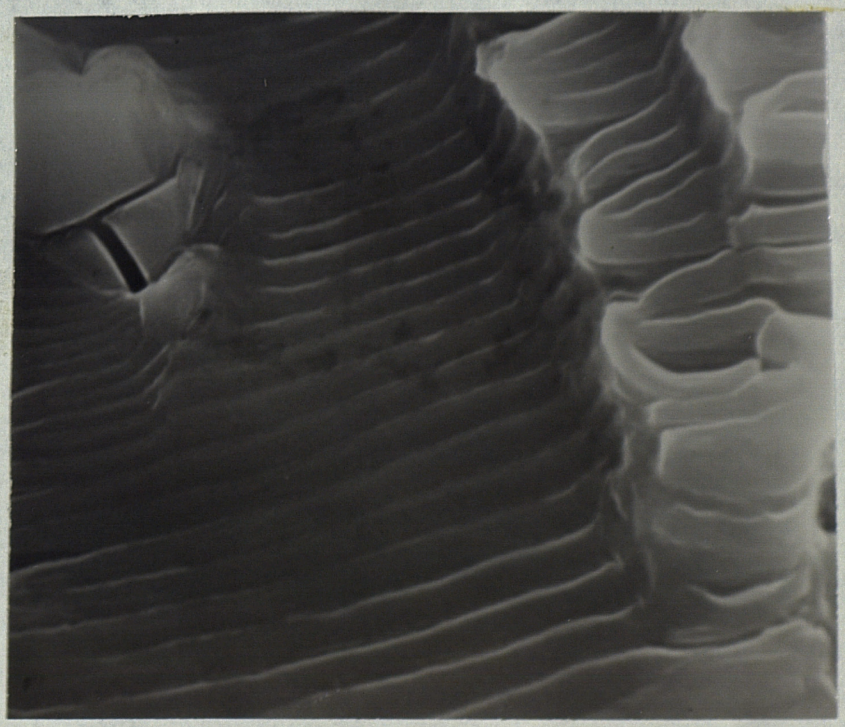

PLATE 2 1000 CYCLE PRESTRAIN BETWEEN S.T. AND AGEING.FATIGUED.(STEREOSCAN x 5.5K)

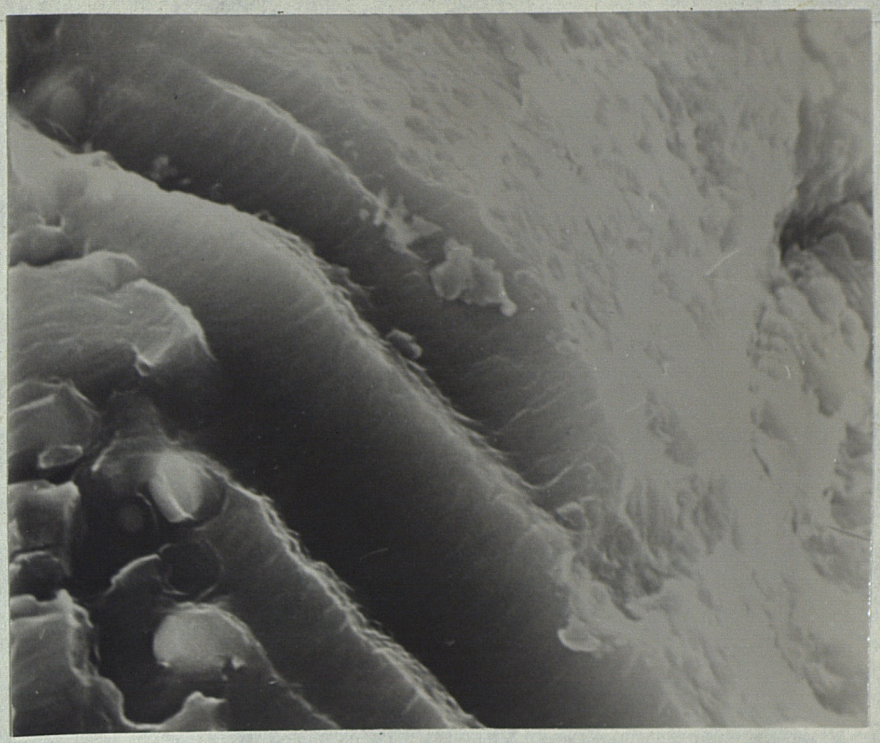

PLATE 3 1000 CYCLE PRESTRAIN BETWEEN S.T. AND AGEING.FATIGUED.(STEREOSCAN x 5.5K)

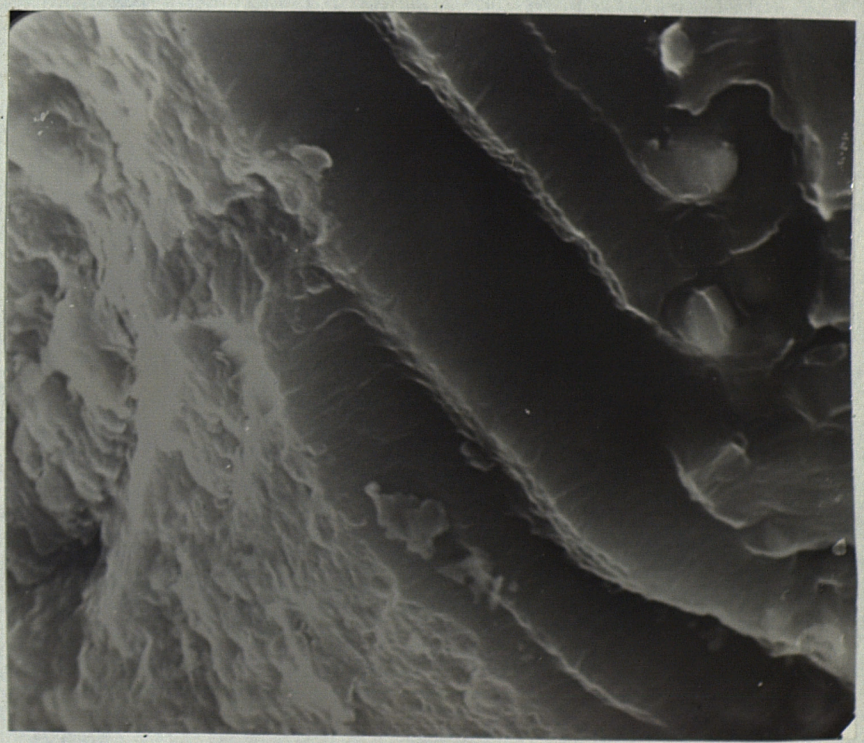

PLATE 4 1000 CYCLE PRESTRAIN BETWEEN S.T. AND AGEING.FATIGUED.(STEREOSCAN x 5.6K)

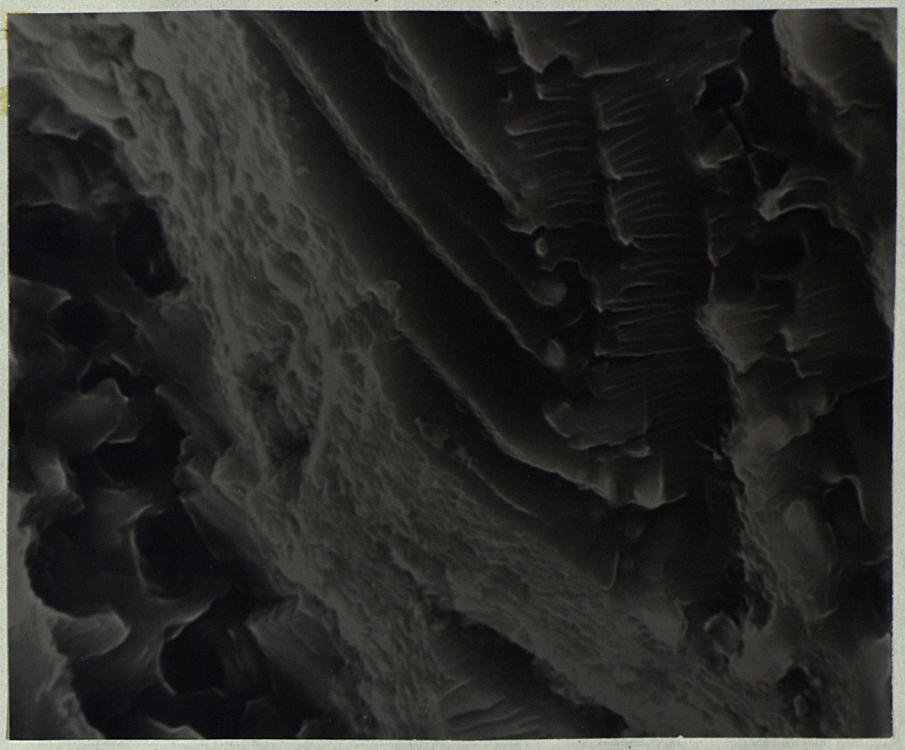

PLATE 5 1000 CYCLE PRESTRAIN BETWEEN S.T. AND AGEING.FATIGUED.(STEREOSCAN x 2.2K)

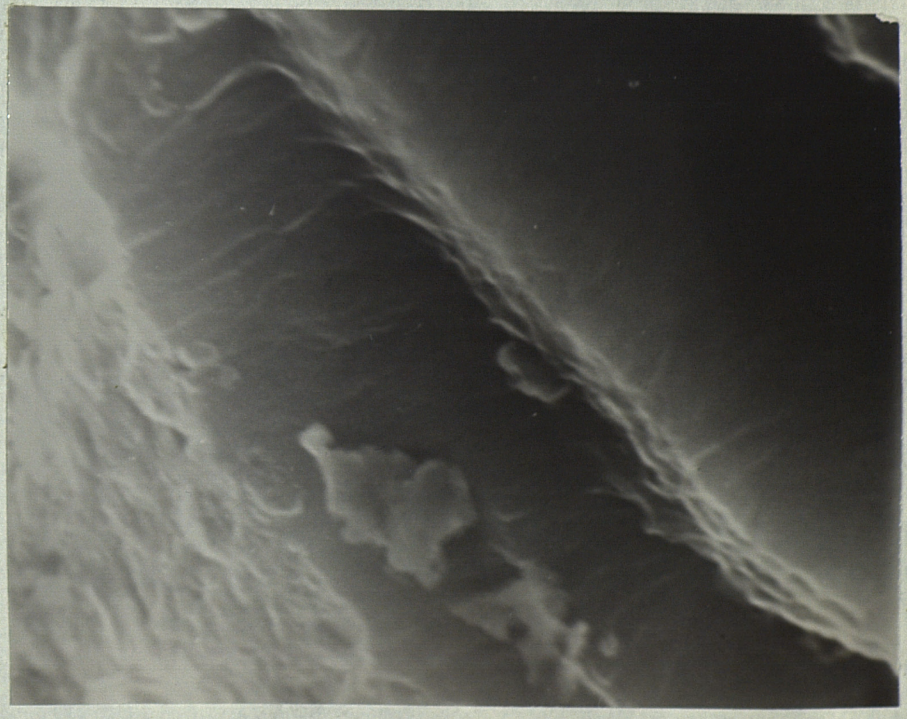

PLATE 6 1000 CYCLE PRESTRAIN BETWEEN S.T. AND AGEING.FATIGUED.(STEREOSCAN x 11K)

PLATE 7 1000 CYCLE PRESTRAIN BETWEEN S.T. AND AGEING. NON-FATIGUE. (ELECTRON MICROGRAPH x 70K)

PLATE 8 1000 CYCLE PRESTRAIN BETWEEN S.T. AND AGEING.NON-FATIGUE.SHOWING SUB-GRAIN BOUNDARY.(ELECTRON MICROGRAPH

PLATE 9 1000 CYCLE PRESTRAIN BETWEEN S.T. AND AGEING.NON-FATIGUE.(ELECTRON MICROGRAPH x 70K)

PLATE 10 1000 CYCLE PRESTRAIN BETWEEN S.T. AND AGEING.NON-FATIGUE.(ELECTRON MICROGRAPH x 20K)

PLATE 11 1000 CYCLE PRESTRAIN BETWEEN S.T. AND AGEING.NON-FATIGUE. (ELECTRON MICROGRAPH x 60K)

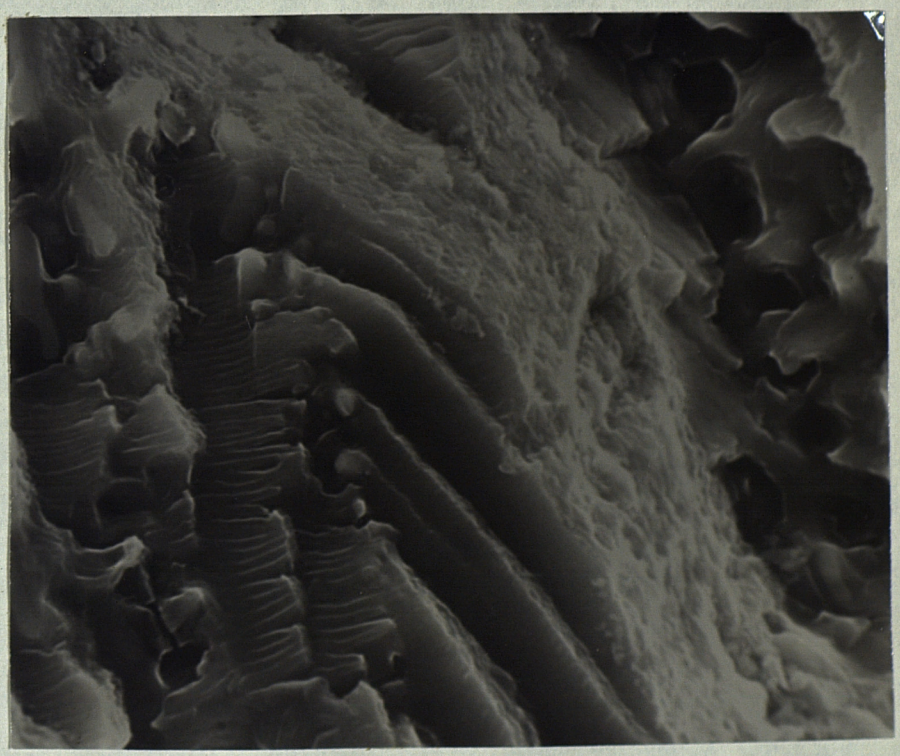

PLATE 12 1000 CYCLE PRESTRAIN BETWEEN S.T. AND AGEING.FATIGUED.(STEREOSCAN x 2.2K)

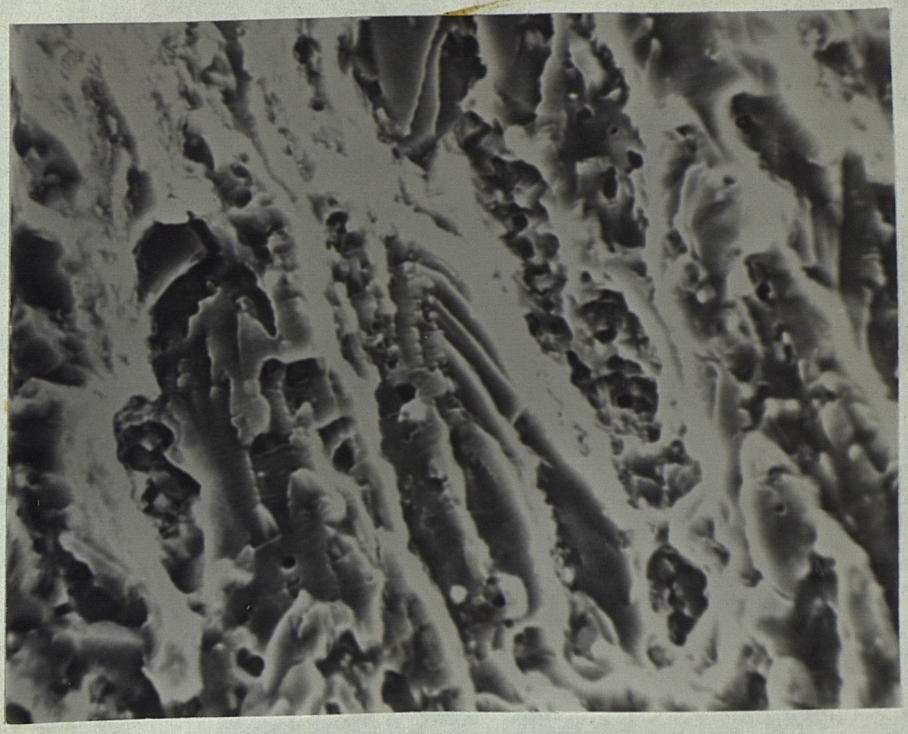

PLATE 13 1000 CYCLE PRESTRAIN BETWEEN S.T. AND AGEING.FATIGUED.(STEREOSCAN x 550)

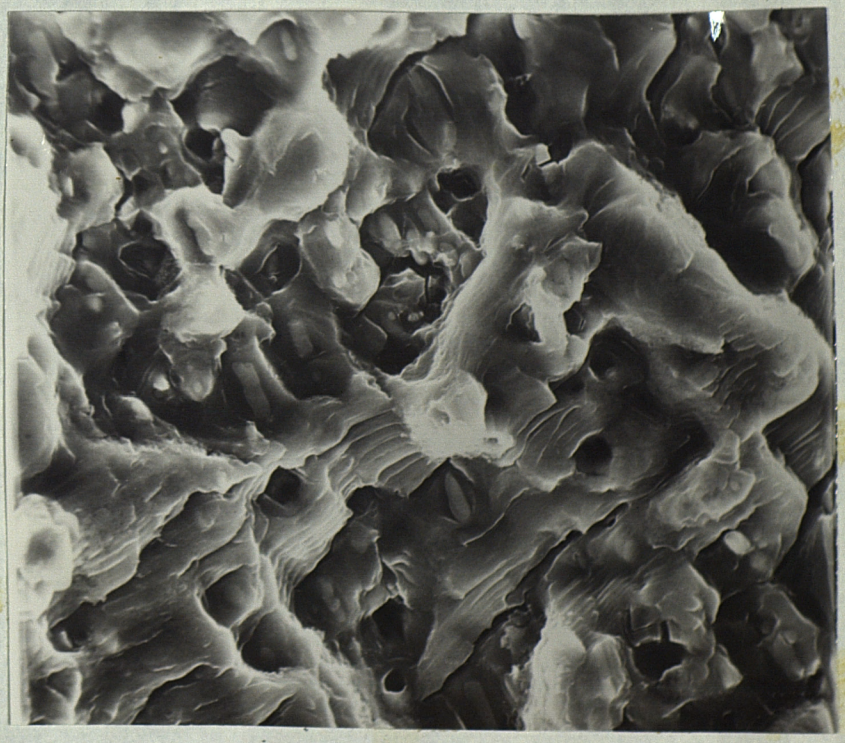

PLATE 14 1000 CYCLE PRESTRAIN BETWEEN S.T. AND AGEING.FATIGUED.(STEREOSCAN x 1.1K)

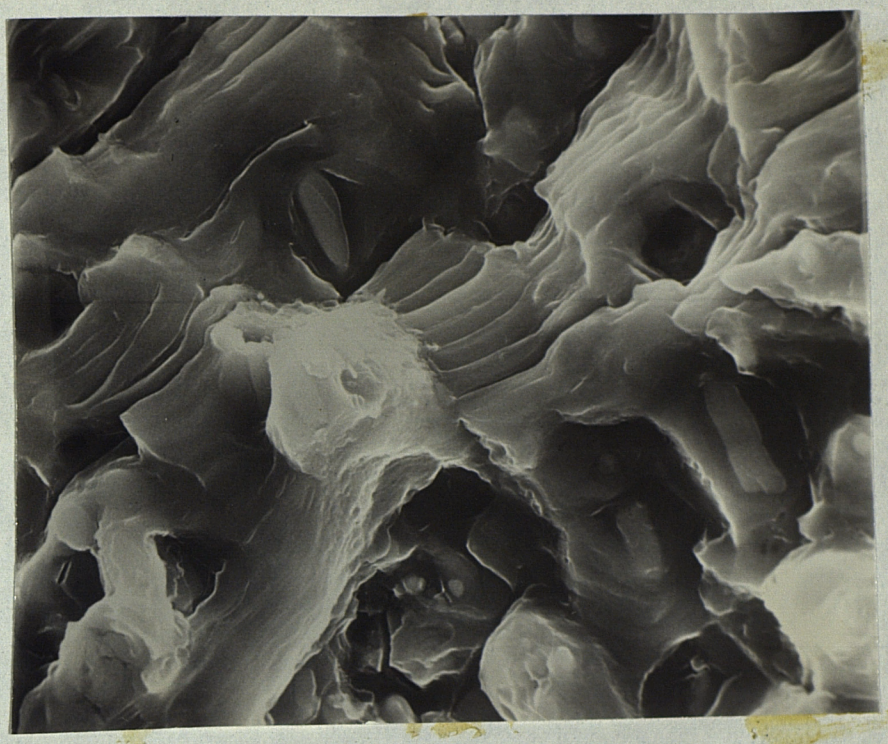

PLATE 15 1000 CYCLE PRESTRAIN BETWEEN S.T. AND AGEING.FATIGUED.(STEREOSCAN x 2.2K)

PLATE 16 1000 CYCLE PRESTRAIN BETWEEN S.T. AND AGEING.FATIGUED.OPTICAL MICROSCOPE.

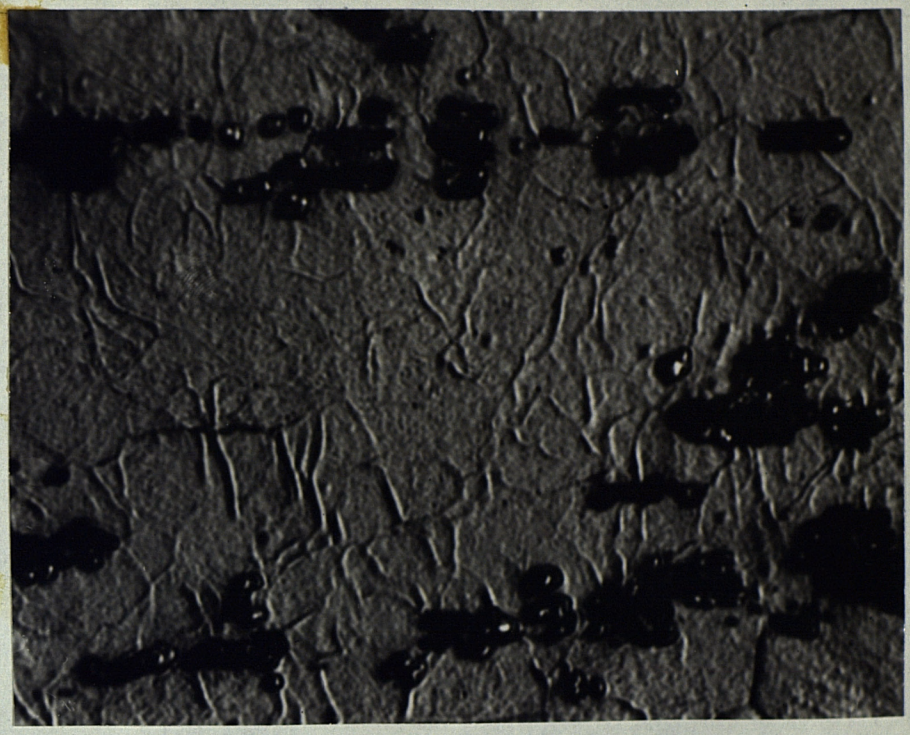

PLATE 17 1000 CYCLE PRESTRAIN BETWEEN S.T. AND AGEING.NON-FATIGUED.OPTICAL MICROSCOPE x 1000.

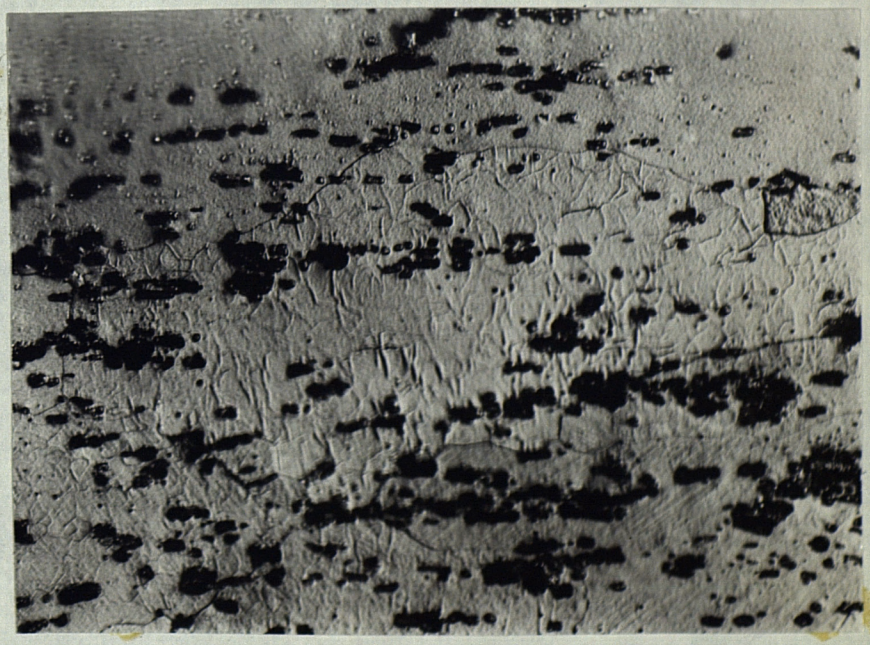

PLATE 18 1000 CYCLE PRESTRAIN BETWEEN S.T. AND AGEING.NON-FATIGUE.OPTICAL MICROSCOPE x 250.

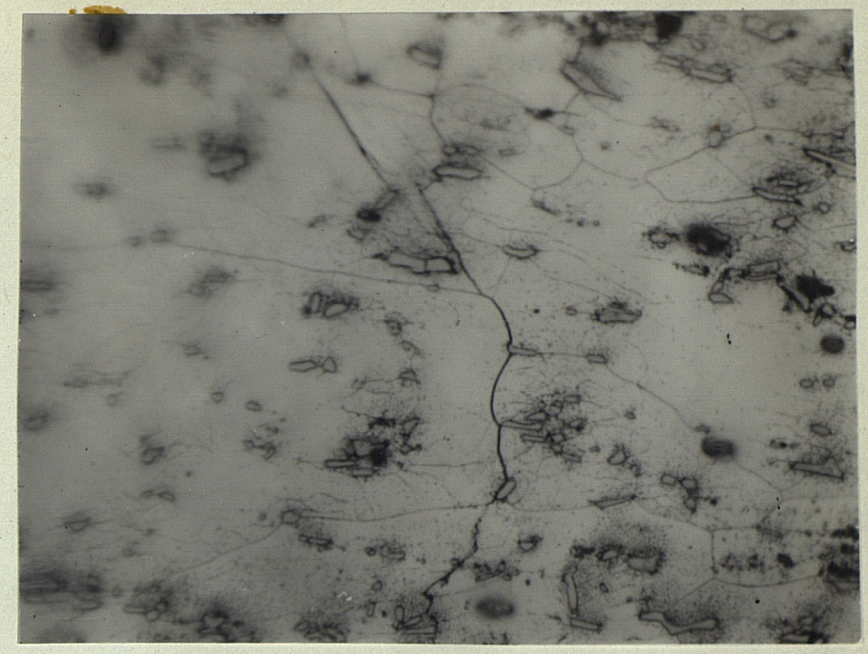

PLATE 19 1000 CYCLE PRESTRAIN BETWEEN S.T. AND AGEING. FATIGUED.OPTICAL MICROSCOPE x 250.

PLATE 20 1000 CYCLE PRESTRAIN BETWEEN S.T. AND AGEING.FATIGUED.(STEREOSCAN x 2.2K)